

Technical Report #33

F/5 SECONDARY SUPPORT

SYSTEM DESIGN

B. Cuerden

March 1998

The University of
ARIZONA[®]
Tucson Arizona

STEWART OBSERVATORY
TUCSON, ARIZONA 85721

March 5, 1998

MEMORANDUM

To: Steve West

FROM: Brian Cuerden /home/bcuerden/f5sec/text/perf.wpd
Technical Services

SUBJECT: F5 Secondary Support System Design

Reference 1. Fabricant, D. McLeod, B. and West, S., "Optical Specifications for the MMT Conversion", Version 5, 3-Nov-96.

SUMMARY

The support performance of the F5 secondary mirror cell is predicted and compared to specifications. Rms WF distortion is 0.0882 waves at 632 nm at zenith and 0.0936 waves rms at 632 n-m in going from zenith to 60 degrees from zenith. Rms surface slope is 0.0233 arc-seconds at zenith and 0.0437 arc-seconds in going from zenith to 60 degrees from zenith as compared to a requirement of 0.091 arc-sec rms at zenith and 0.138 arc-sec at 60 degrees from zenith. Structure functions at zenith and 30, 45 and 60 degrees from zenith have been calculated and are below the allowable structure functions.

INTRODUCTION

The secondary support system consists of 24 lateral supports and 36 axial supports, three fixed axial positioners and three fixed tangential positioners. Loads are sensed at the fixed positioners and are held to a low value (0.25 lbs) by adjusting the pressures in three zones of axial and one zone of lateral supports. At each of the 66 locations on the mirror where a force or position constraint is applied, there is the possibility of inadvertently applying 5 force and moment components in addition to the intended force, and the intended force may vary from its ideal value. For example, at an axial support we wish only to apply a force parallel to the optical axis, F_z , but because of small misalignments, offsets, friction or stiffness in the axial support system, we can expect to obtain in addition F_x , F_y , M_x , M_y and M_z components. Much of the design of the supports is involved in minimizing the magnitude of these extraneous forces and in

making the intended force (F_z in the example) sufficiently accurate to maintain good surface figure.

The magnitude of these error forces can be estimated and the effect of each individual component can be predicted. Since there are $6 \times 66 = 396$ such components, and since most of them can be considered to be statistically independent of the others, the net effect of all these components can be obtained by RSS'ing the effects of each force.

Some of the error forces are not statistically independent. If the axial supports have stiffness, cell bending will result in a support force distribution that induces astigmatic bending of the mirror. With the finite number of axial supports we have, the probability of obtaining a random distribution of error forces having an astigmatic component is too high to ignore (astigmatic bending is the softest mode of deformation of the mirror and we must be particularly careful to keep force error small enough to prevent this deformation mode). The effects of systematic force sets are calculated by FEM analysis and RSS'd into the statistically independent results described above.

Gravity deflections are also included in the "support" term of the secondary error budget. Gravity deflections are calculated by FEM. Since the mirror is figured to meet its polishing budget when supported axial supports identical to those used in the telescope cell, the zenith pointing gravity sag attributable to the mirror support is zero (already included in the polishing). As the LOS moves away from zenith, the mirror distorts due to the change in gravity and the shift in support forces from the axial supports to the laterals. This is modeled by applying the gravity and support force changes that occur in moving from zenith to some elevation angle to the finite element model. These results are RSS'd in with the other sources of distortion to arrive at a net result for a particular telescope orientation.

Surface figure can be expressed as rms or P-V surface or wavefront distortion, FWHM, encircled energy or as a structure function. All these can be combined using the RSS operation although the details of combining structure functions may not be obvious and are described in Appendix A.

The calculations outlined above were performed on the MMT F5 Secondary Mirror using an initial set of estimated error forces. The initial results exceeded the distortion requirements and the component force effects were searched to find damaging terms. Once a particular component was identified as a major contributor to distortion, the design was changed to reduce the magnitude of that force component. The results of this operation are a performance prediction that meets the requirements for the support system and a large number of design constraints on the secondary support system components. Much of these design constraints are in the form of positional and alignment tolerances. These are identified in Appendix B.

This report describes the results of evaluating and combining a large number of finite element solution sets in accordance with the general procedures outlined above. Due to the large volume of data being processed, the compilations are performed by a computer program using data files

generated by other computer programs. Details of this procedure and of the results obtained are described in this report and its Appendices.

DISCUSSION

Secondary Support System Requirements

The F5 secondary support requirements are defined in Reference 1 section 6.2.1. The table lists a support allocation r_o of 141 cm for the F5 secondary. The corresponding encircled energy requirement is 0.071 arc-sec FWHM. These requirements apply for zenith pointing. At angles, θ , from zenith, the allowable structure function is $141 \cdot \cos(\theta)^{0.6}$ cm and the required encircled energy requirement is $0.091/\cos(\theta)^{0.6}$ arc-sec rms ($0.071/\cos(\theta)^{0.6}$ FWHM).

Table 1 Summary of f9 Secondary Support Requirements

Requirement	Value	Specification
Rms Surface Slope	$0.091/\cos(\theta_d)^{3/5}$ arc-sec	Ref 1, Sections 6.2.1, 5.53 and 4.2
Structure Function, r_o , cm	$89 \cdot \cos(\theta_d)^{3/5}$ cm	Ref 1, Section 6.2.1

The encircled energy requirement for the secondary support is
 $0.017 \cdot 4.13 \cdot 1.28 \cos(\theta)^{0.6}$ FWHM

Cell Configuration

The cell configuration is shown in Appendix F. There are 36 pneumatic axial supports in three circles of 6, 12 and 18 supports. Each support in the outer circle provides 80% of the force of a support in the inner two rows. The axial supports are grouped into three zones of 120 degrees extent. There are 30 pneumatic lateral supports in two circles, an inner row of six and an outer row of 24. Each support in the inner circle provides 70% of the force of a support in the outer row. The position of the mirror is fixed by three axial rods attached to the back and three tangent rods attached to the OD. Pressures in the three axial zones and in the lateral supports are controlled to minimize reaction forces in the fixed locators. Secondary position is maintained by three fixed axial points and by three tangent constraints in the cg plane. Five of the fixed points are equipped with load cells (loading along the elevation axis and torque about the LOS are not controlled).

Analysis Procedure

An ANSYS finite element models of the f9 secondary was used as shown in Figure 1. This model is estimated to be accurate to better than 20% so the mass has been adjusted upward 20% to ensure conservatism in the gravity sag results. ANSYS displacement results were processed to remove translation tilt and power after which the rms and P-V deviations, the maximum slope deviation and the structure function was computed. Load cases considered are summarized in Table 2.

Table 2 Summary of Mirror Support Load Cases

Gravity	1 g, Zenith to 60° el, Zenith to 45°, zenith to 30° el and horizon pointing.
Unit Load	Fx, Fy, ...Mz loads were applied to representative support locations. One location on the inner and outer axil support locations and one location on the OD (tangent supports/ lateral force actuator location). These results were used to compute the effects of random mounting force errors. Error forces are estimated in Appendix B. Effects of error forces is obtained by RSS'ing individual effects (see Appendix A, section 2.2.2).
Other	The effects of non-random force distributions (see Appendix A, section 2.2.3 and Appendix B section B.7) were also investigated. Of primary concern is the effect of a $\sin(2\theta)$ axial force distributions which generate more deflection than randomly distributed forces of the same magnitude.

A detailed description of the methods employed to evaluate and combine these load cases may be found in Appendix A. The magnitude of error forces are calculated in Appendix B.

RESULTS

In Tables 3 and 4 the total effect of gravity loading and spurious error forces is obtained by RSS'ing all effects. Table 3 is a summary of the net performance reported in Table 4a and 4b and Tables C2 and C3 in Appendix C. The random error effects are based on the error forces estimated in Appendix B. These error force estimates are in part based on the dimensional tolerances specified in Appendix B. Structure function plots are provided as Figures 2 to 5. In Appendix D structure function plots are provided that define the contribution to the total error of selected groups of error sources.

Table 3 MMT F/5 Secondary Support Performance, Various Orientations

Orientation	WF Distortion, Waves at 0.632 μ -m	RMS Surface Slope arc-seconds rms	Reference Figure for Structure Function
Zenith Pointing	0.0882	0.0233	Figure 2
30° From Zenith	0.0901	0.0286	Figure 3
45° From Zenith	0.0916	0.0351	Figure 4
60° From Zenith	0.0936	0.0437	Figure 5

Table 4a F5 Secondary Surface Performance Zenith Pointing

Waves are 0.632 μ -m
See Addendum 1 for error force estimates and backup data

Load Case	Rms Surf Distortion		Max Slope arc-sec rms
	μ -inch	WF, λ	
Gravity, Zenith to Indicated Elev	0	0	0
Lateral and Axials Fz Astig. Cell Bend	0.284	0.0228	0.006
Axials Fz Astig, random	0.164	0.0132	0.004
Laterals Fz Astig, random	0.214	0.0172	0.005
Random Force Errors	1.026	0.0824	0.0216
RSS Total =	1.0982	0.0882	0.0233

Table 4b F5 Secondary Surface Performance 60 Degrees From Zenith

Waves are 0.632 μ -m
 See Addendum 1 for error force estimates and backup data

Load Case	Rms Surf Distortion		Max Slope arc-sec rms
	μ -inch	WF, λ	
Gravity, Zenith to Indicated Elev	0.390	0.0313	0.037
Lateral and Axials Fz Astig. Cell Bend	0.284	0.0228	0.006
Axials Fz Astig, random	0.164	0.0132	0.004
Laterals Fz Astig, random	0.214	0.0172	0.005
Random Force Errors	1.026	0.0824	0.0216
RSS Total =			
	1.1654	0.0936	0.0437

A cell structure model has been developed and used to evaluate the cell bending deflection. Cell bending deflections are used in Appendix B, section B.7.2 in assessing the astigmatic loads applied to the mirror by cell deflections acting through the actuator stiffness.

Wind loadings and there effects on surface distortion are evaluated in Appendix G.

CONCLUSIONS

The secondary surface figure requirements have been met. Appendix B contains numerous requirements on the cell design that must be satisfied in order to achieve the desired level of support performance.

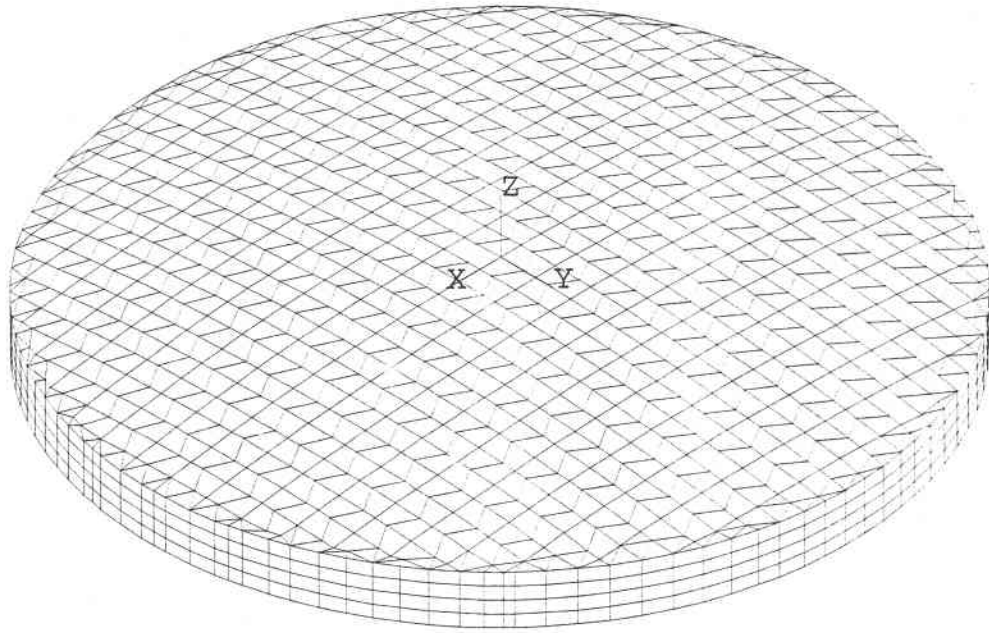


Figure 1a
MMT F5 Secondary

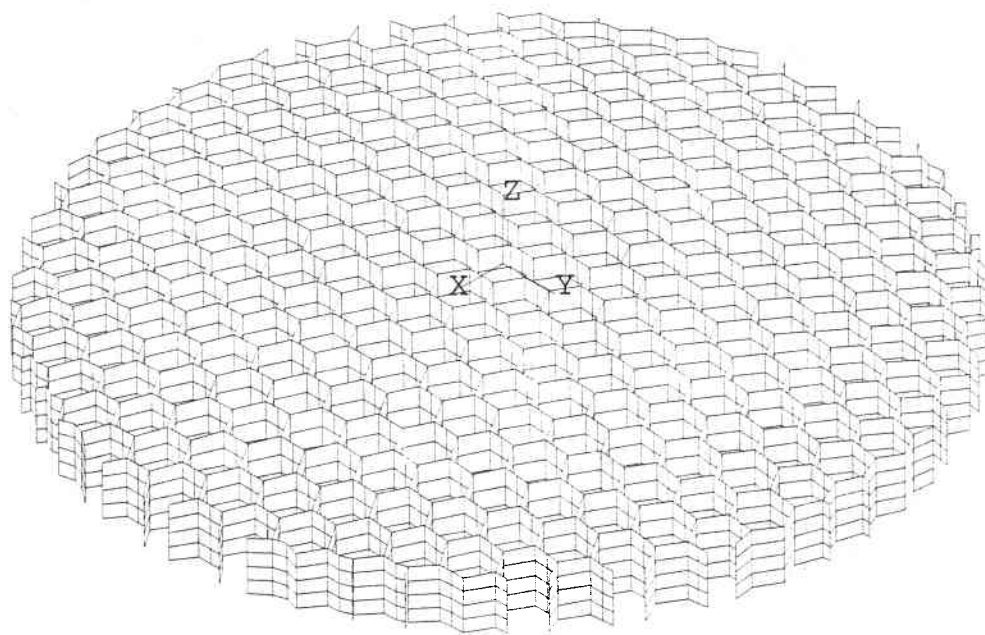


Figure 15
MMT F5 Secondary

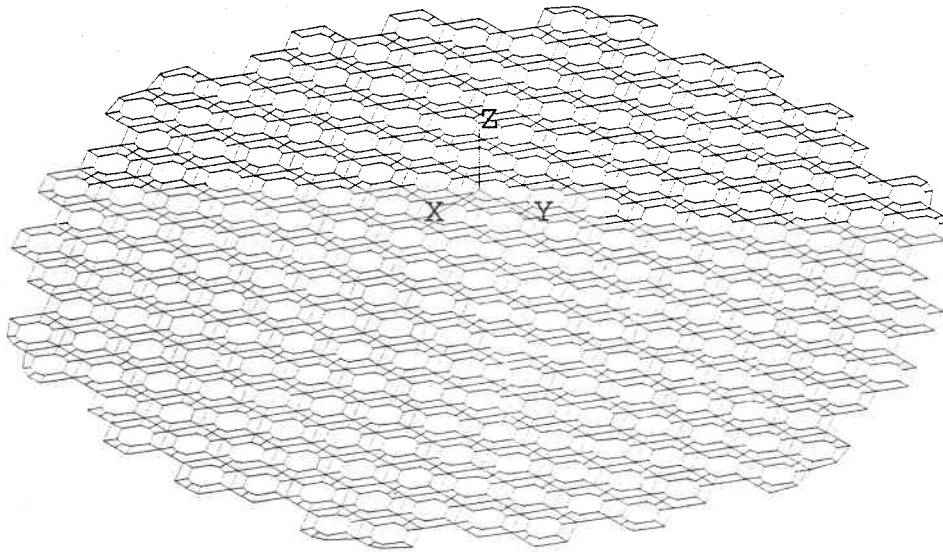


Figure 1c
MMT F5 Secondary

Figure 2 Structure Function, MMT f/5
Zenith Pointing

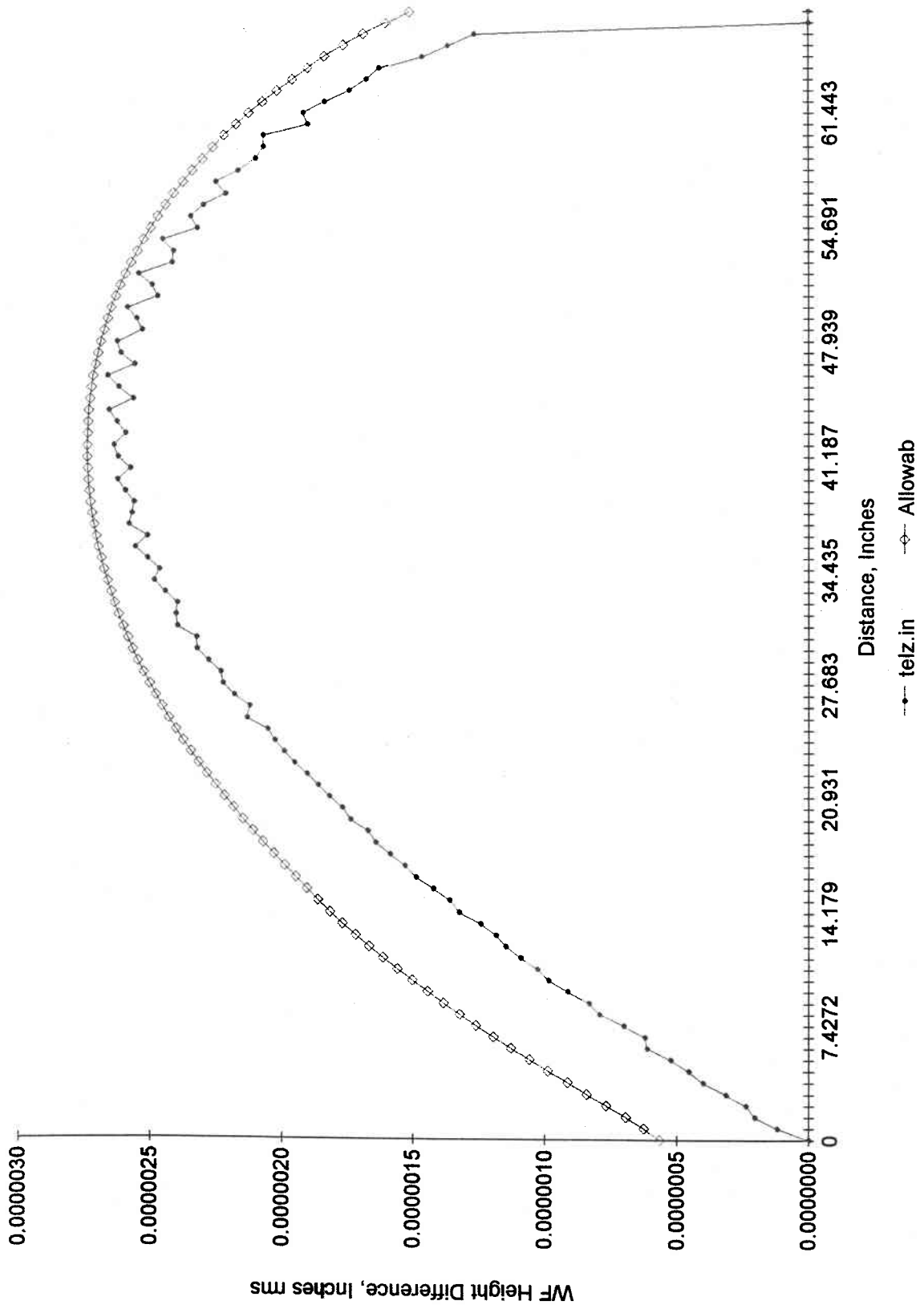


Figure 3 Structure Function, MMT f/5
 LOS 30 Degrees from Zenith

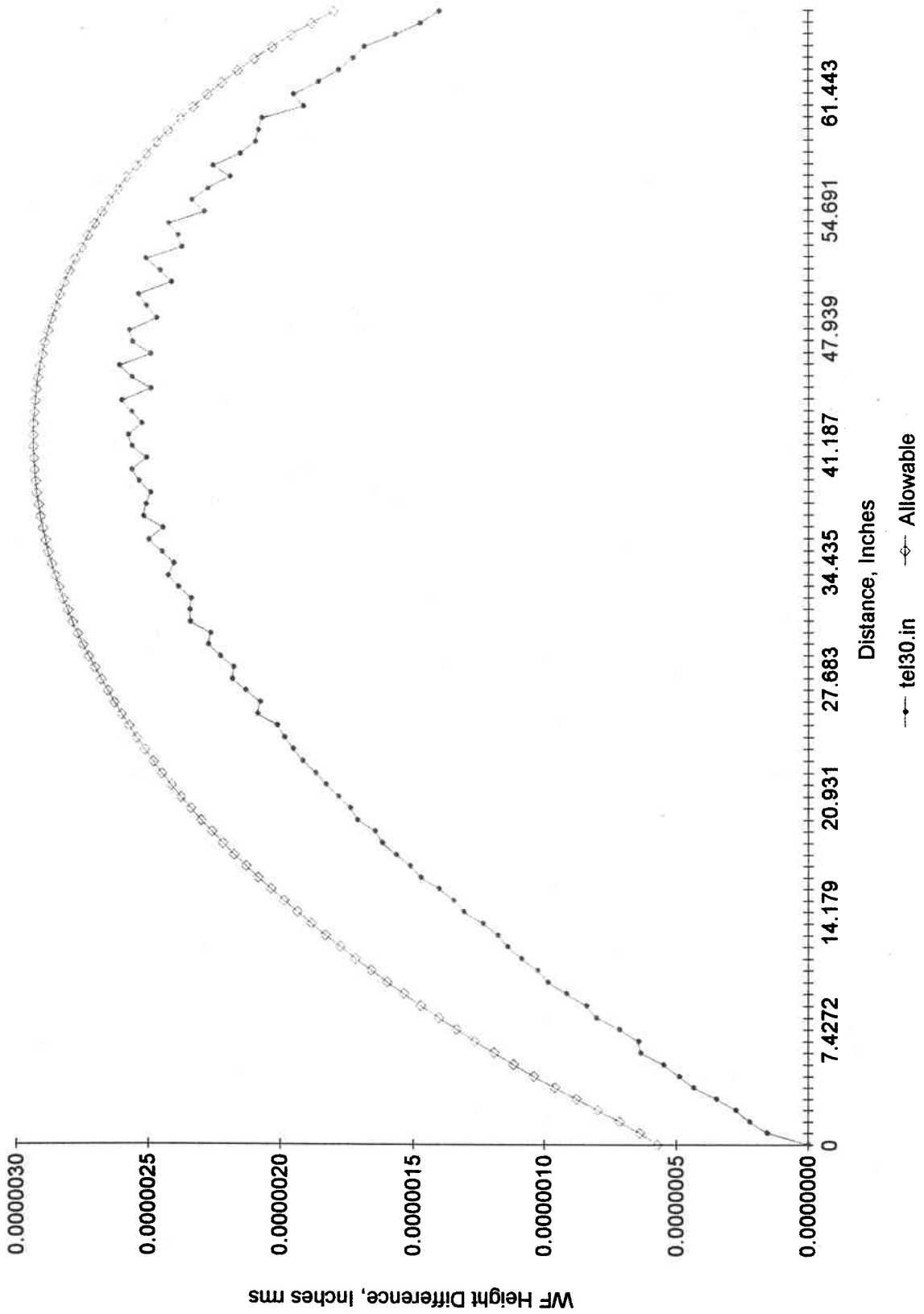


Figure 4 Structure Function, MMT f/5
 LOS 45 Degrees from Zenith

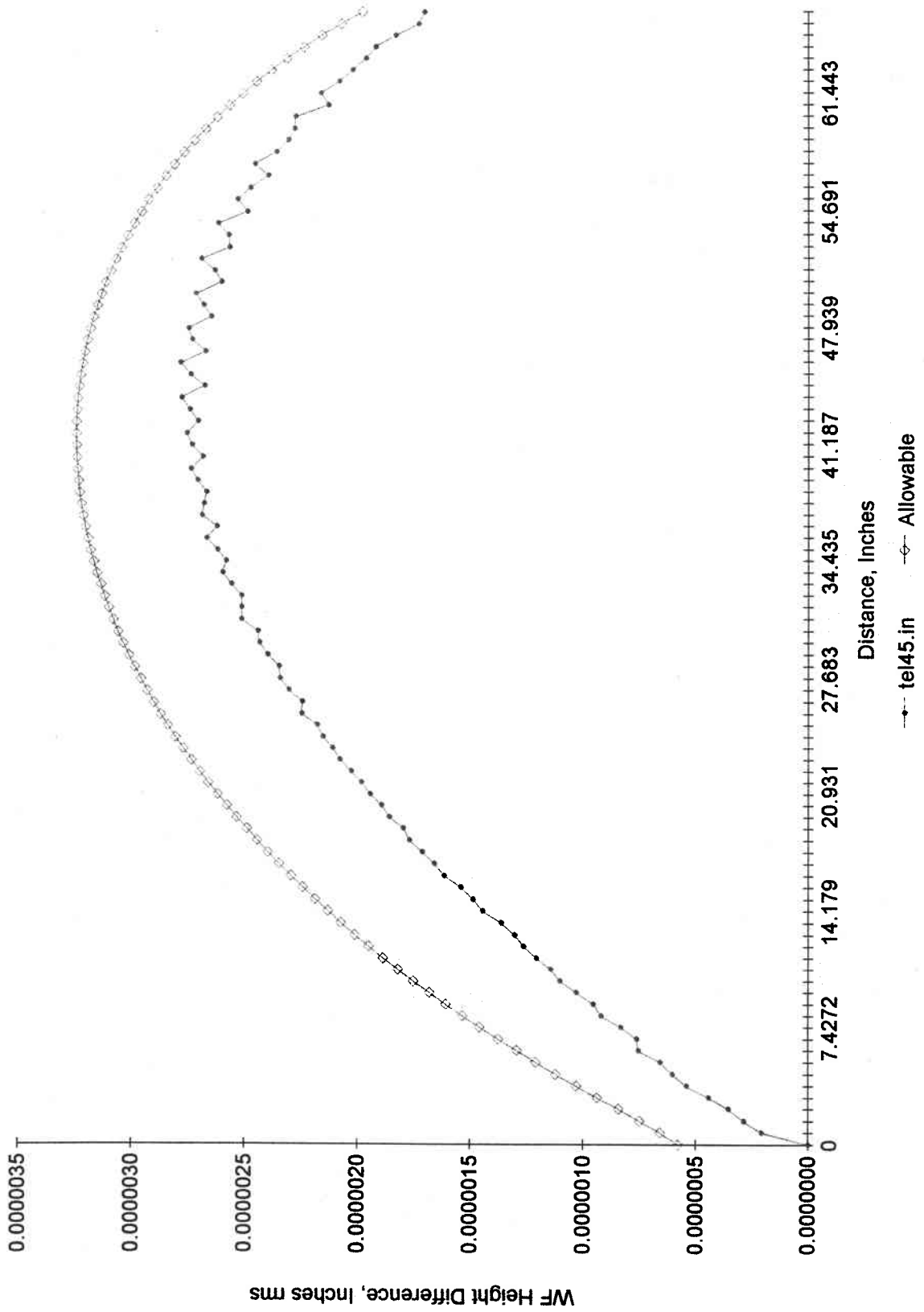
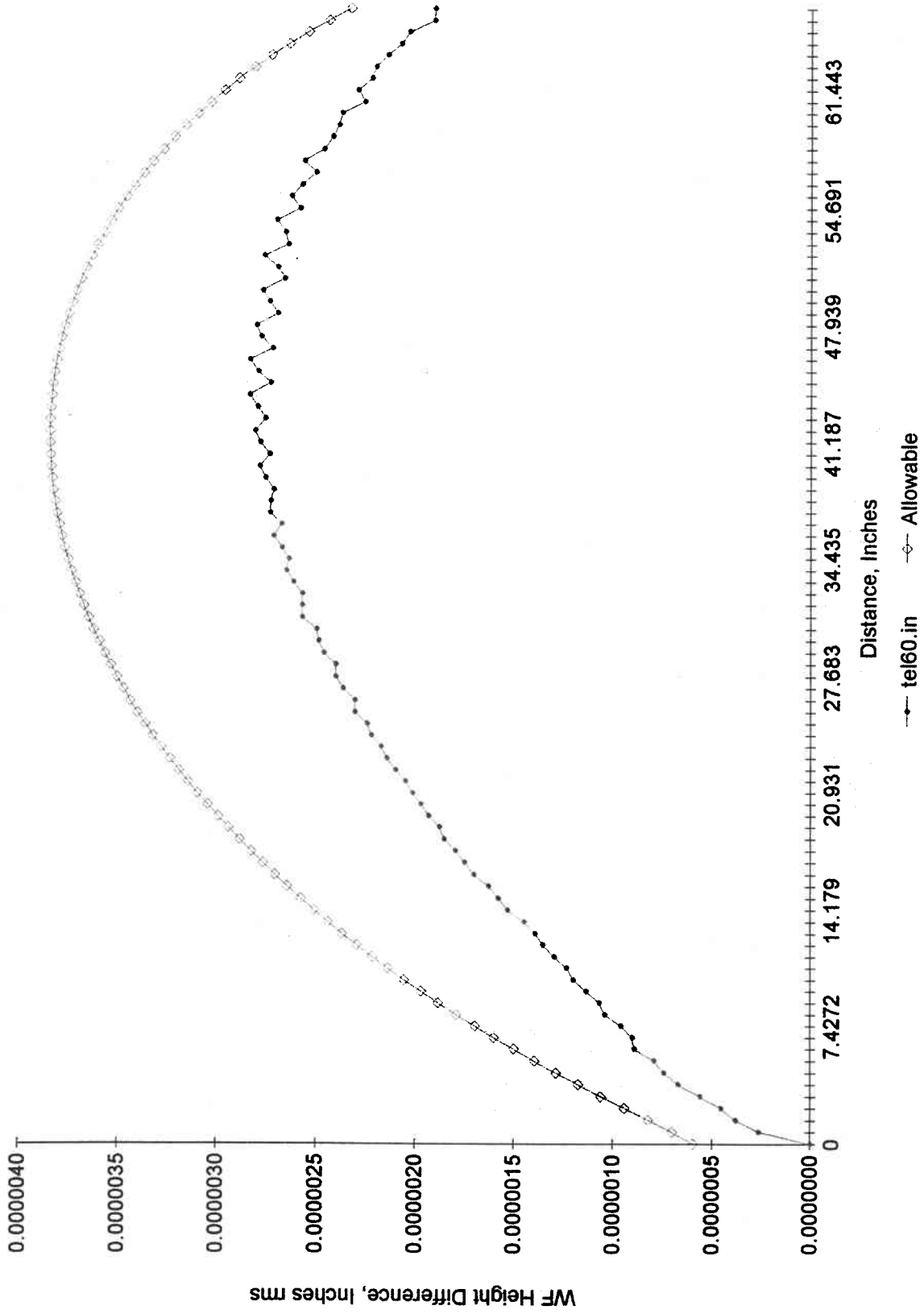


Figure 5 Structure Function, MMT f/5
 LOS 60 Degrees from Zenith



APPENDIX A SUPPORT PERFORMANCE ANALYSIS METHODOLOGY

This Appendix discusses in a general way the procedures used to demonstrate that the support design can limit the optic's surface deformation to less than that allowed by the specified structure function.

A.1.0 Structure Functions

A.1.1 The Allowable Structure Function

Reference: Hill, J. M., "Error Budget and Wavefront Specifications for Primary and Secondary Mirrors", Technical Memo UA-94-01, Aug 26, 1994

The surface of the optic is required to meet distortion limits specified as a "structure function" (see reference Section 1.0 to 1.4). The structure function allowable (for a secondary mirror) is:

$$\delta^2(x) = 2\sigma^2 + \left(\frac{\lambda}{2\pi}\right)^2 * 6.88 \left(\frac{Cx}{r_0}\right)^{\frac{5}{3}} * \left[1 - 0.975\left(\frac{Cx}{D}\right)^{1/3}\right]$$

Where:

$\delta(x)$	is the permissible rms wavefront height difference of two points separated by distance, x (the permissible surface height difference is half this for normal incidence).
σ	is the rms deviation from the mean wavefront due to scattering
λ	is the reference wavelength
C	is the ratio of primary to secondary beam diameter
x	is the distance between points at which the height difference is computed
r_0	is the parameter that defines the allowable magnitude of the structure function. r_0 decreases away from zenith as $r_0(z) = r_0(0) * \cos(z)^{0.6}$ z is zenith angle, 0 at zenith.
D	is the telescope aperture diameter

The C in the term $(Cx/r_0)^{5/3}$ is the scaling factor for pupil size. This factor may be included in the secondary error budget in which case it must not be included again in this term.

Note that all these variables must have consistent units.

A.1.2 Calculation of the Structure Function of a Distorted Surface

Finite element results for the optical surface distortion consist of a set of displacements at discrete points (nodes) on the optical surface. The structure function is computed as the rms normal displacement difference between nodes that are approximately the same distance apart. Since the nodes may not be uniformly distributed, values are weighted with respect to area. Before calculating the structure function, displacements, tilts and power are removed from the surface normal displacement solution. The calculation of the structure function then proceeds as follows:

For two nodes, i, j , separated by some distance, x , and having associated areas, A_i and A_j :

Compute the area weighted height difference, $\delta_{ij}(x)$ and the average area, A_{ij} :

$$\delta_{ij}^2 = 4 * (U_{z_i} - U_{z_j})^2 * \frac{(A_i + A_j)}{2}$$

Where the factor of 4 converts from surface height difference squared to wavefront height difference squared.

$$A_{ij} = \frac{A_i + A_j}{2}$$

Sum these values into bins depending on the distance between nodes, x_{ij} , so that:

$$\begin{aligned} \text{Sum}_k(\delta^2) &= \sum \delta_{ij}^2 && \text{for } L_k < x_{ij} \leq L_{k+1} \\ \text{Sum}_k(A) &= \sum A_{ij} && \text{for } L_k < x_{ij} \leq L_{k+1} \end{aligned}$$

Where L_k are reference lengths for 1% of the secondary diameter to the secondary diameter in 1% increments

$$\delta_k = \sqrt{\frac{\text{Sum}_k(\delta^2)}{\text{Sum}_k(A)}}$$

δ_k = the calculated value of the structure function for distance L_k .

The δ_{ij} values are computed for all unique node pairs ($\delta_{ii}=0$ and is ignored and $\delta_{ji}=\delta_{ij}$ and so need not be included).

A.1.3 Combining Structure Functions

Calculated structure functions on the same surface are combined by RSS'ing the δ_k values for the various cases being combined to yield a new set of δ_k values.

A.2.0 Calculation of Net Mirror Distortion Attributable to the Support System

The section above describes how the structure function is calculated from a finite element displacement solution, how results from multiple solutions can be combined, and how to calculate the maximum allowable value of the structure function.

In this section, the load cases that must be included in the total solution are discussed as are methods for reducing the number of cases requiring evaluation by taking advantage of symmetry.

A.2.1 Gravitational Deflection

The support system is required to meet its requirements for all operational orientations of the mirror. For secondaries tested nadir pointing on their operational supports gravity sag for this orientation is polished out. As the horizon pointing condition is approached, the mirror surface will exhibit both the lateral gravity distortion and the nadir pointing distortion. The finite element case that models this effect is obtained by applying the following gravitational accelerations:

$$\begin{aligned} \text{Surface normal gravity} &= (\cos(\theta_e)-1)*g \\ \text{Lateral gravity} &= \sin(\theta_e)*g \end{aligned}$$

$$\begin{aligned} \text{Where: } \theta_e &= \text{the elevation angle (zero at the horizon)} \\ g &= \text{gravitational acceleration} \end{aligned}$$

The structure function for various orientations of the telescope must be evaluated using separate finite element load cases.

A.2.2 Support Force Errors

Mirrors are generally supported on a kinematic support with auxiliary forces applied to reduce surface distortion. The kinematic support often takes the form of six rods each preventing

motion along a particular direction and positioned to constrain each of the six rigid body degrees of freedom. One example of this is three axial supports on the back and three tangent rods on the OD of the mirror. Another example is three bipods on the back of the mirror (Stuart platform). The rod elements are required to constrain motion only along their length but they also introduce small error forces normal to the rod axis and moments about and normal to the rod axis. These error forces may result from frictional or elastic effects depending on the rod construction. Elastic error forces are more likely to be constant or at least predictable than frictional forces which is an advantage in an actively corrected optical system. Friction error forces can be smaller than elastic forces, particularly if rolling element bearings are employed.

The auxiliary forces are usually intended to be a single force component acting in a particular direction at a particular location. The method of interfacing the force actuator to the mirror results in small error forces and moments in addition to the intended force. In addition, the magnitude of the applied force will differ from the intended value by some small amount.

A.2.2.1 Estimating Support Force Errors

No general procedure for estimating error forces can be given since each case is different. Some special purpose programs are available for flex rod analysis and there is some data for Bellafram diaphragms (spring rate and hysteresis). However the error forces are calculated, all six possible force components at each mirror attachment should be evaluated.

A.2.2.2 Random Support Force Errors

Random support force errors are those which are not correlated. Error forces resulting from differential thermal growth of the cell and mirror will not usually be random but errors resulting from installation position errors of individual supports could well be random.

Random support force errors can be evaluated by sampling the effects at one location and using those results at all similar locations. For example, if a mirror is supported at three points on the OD, the structure functions resulting from F_x, F_y, \dots, M_z can be obtained at one of the locations and the net effect at all three locations obtained by RSS'ing the structure function values at each distance for each force component at each location, i.e.;

$$\delta_i^2 = N[\delta_i^2(F_x) + \delta_i^2(F_y) + \dots + \delta_i^2(M_z)]$$

- Where:
- δ_i is the i^{th} value of the structure function (corresponding to the i^{th} distance)
 - N is the number of similar locations (including the first location in the count)
 - $\delta_i(F_x)$ is the i^{th} value of the structure function due to F_x being applied at the representative location.

A.2.2.3 Non-Random Errors

These are sets of forces acting on the mirror that are correlated in some way. Examples are forces that result from differential thermal growth or a displacement of the mirror relative to the supports. These effects tend to produce force sets that have net radial, lateral or astigmatic components. Force sets that generate the low order flexural modes of the mirror can yield deflections that are much larger than would be predicted using the random support force analysis procedure above. Non-random force sets must therefore be evaluated by estimating the magnitude and distribution of the non-random sets and applying them as separate load cases to the finite element model. Section B.7 includes a discussion of the probability of getting an astigmatic force distribution of a given magnitude in a finite set of supports.

A.2.2.4 Totalling the Effects of all Error Sources

Gravity, random and non-random structure function errors are combined by RSS'ing the results of sections 2.2.1, 2.2.2 and 2.2.3. Specifically;

$$\delta_{Total} = \sqrt{\delta_g^2 + \delta_{Random}^2 + \delta_A^2 + \delta_B^2 + \dots}$$

- Where:
- δ_{Total} is the net support system structure function
 - δ_g is the structure function for gravity at a particular elevation angle (ref. 2.2.1).
 - δ_{Random} is the net random error force structure function (ref. 2.2.2)
 - $\delta_A, \delta_B, \text{etc}$ are the non-random cases (ref 2.2.3)

APPENDIX B Error Force Estimates

Mirror Mass Properties (As Modeled using 1.2* nominal material density)

Weight = 836.48 lbs
CG = (0,0,-4.0204) origin at face mid-plane at vertex

Mass Moments of Inertia

	About Origin	About CG	Units
I _{xx} =	655	620	in-lb-sec ²
I _{yy} =	655.5	620.5	in-lb-sec ²
I _{zz} =	1216	1216	in-lb-sec ²

B.1 Elastomeric Diaphragm Characteristics

The supports are built around a Bellofram class 4 diaphragm 1.37 x 1.19 x 1.37 height, "C" sidewall thickness, and an .090" convolution (aslightly smaller unit is used for the outer row of axial supports). Prototype actuators containing these diaphragms were tested to measure thier stiffness and hysteresis properties.

B.1.1 Test Method

Axial stiffness (and other support parameters) were measured by hydraulically connecting two of the 1.37" cylinder diameter units. Weights were applied to each support producing a hydraulic seesaw where pushing down on one support causes the other support to rise. A micrometer head pushing through a 25 lb load cell was used to displace one of the supports enabling a precise measurement of the force required to displace the loaded support.

B.1.2 Hysteresis Measurements

Displacing the pair of supports 0.005" produces a force change that starts at about 0.2 lbs (0.1 lb/support) and decays down to 0.152 lbs (0.076 lbs/support) after 6 minutes. This behavior is exhibited in Figure B1. The force change has been reported to continue to decay over many hours but this effect has not been quantified on these supports.

Diaphragm supports exhibit stiffness and hysteresis. The hysteresis is shown in Figure B2. The supports were displaced from +.475 to .45 to .43 to .45 to .47 continuing with decreasing amplitude to ± 0.005 " amplitude cycles. Previous work had indicated that a decreasing amplitude displacement cycle of this type would erase the effects of hysteresis giving a force at a position that was independent of the displacement history. This was found to be only partially true. Figure B3 shows the results of performing the

Figure B1 Step Response, 0.005" STEP

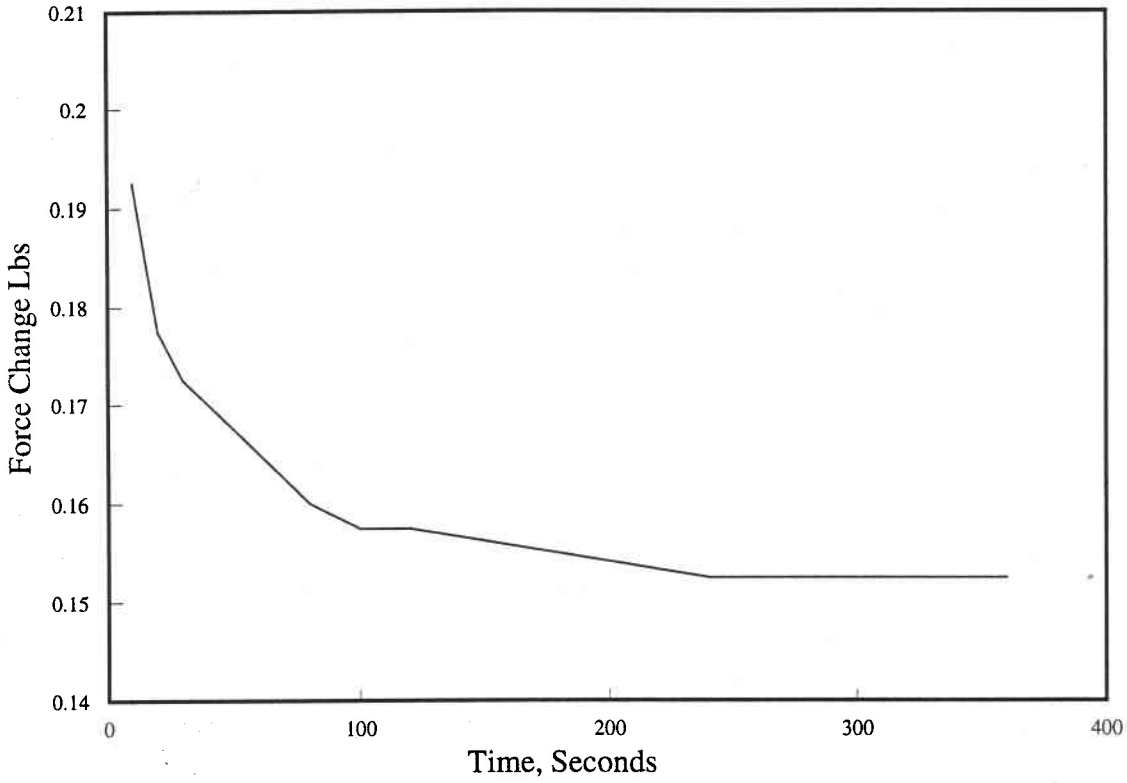


Figure B2 Initial Shakedown

Decreasing Amplitude Cycles

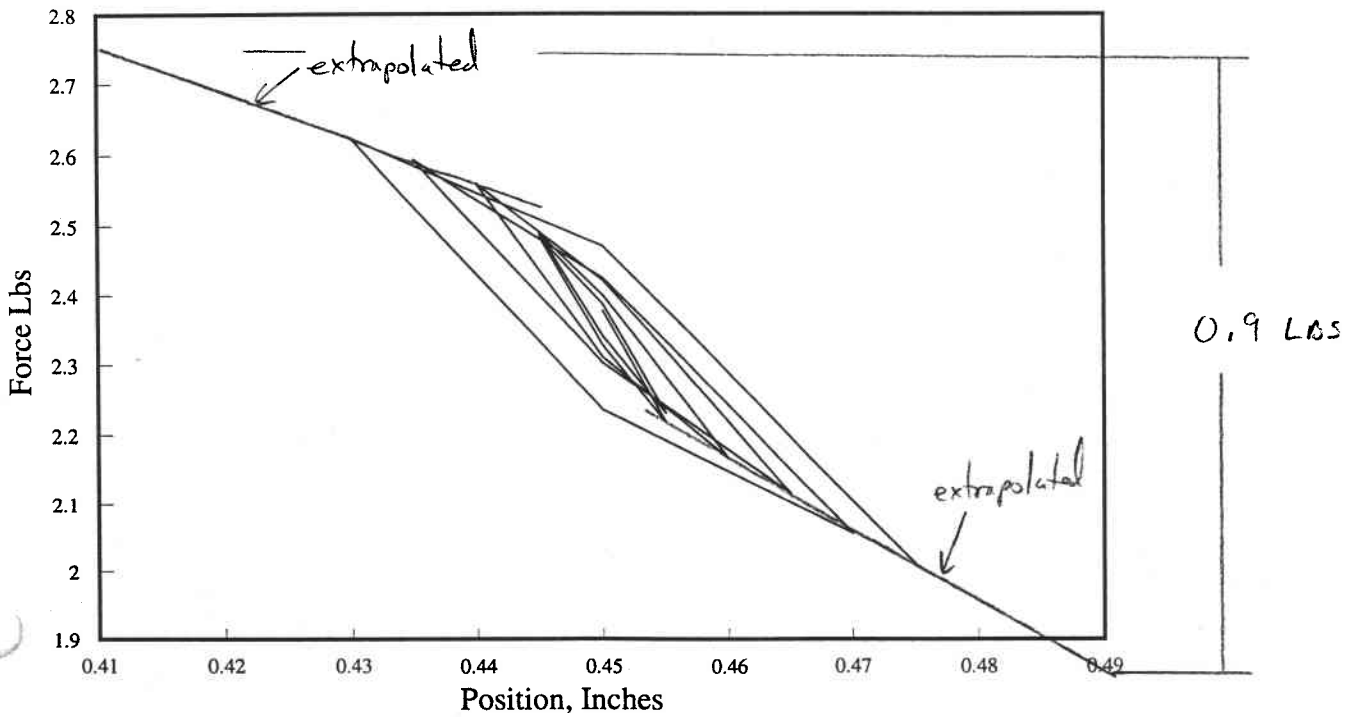
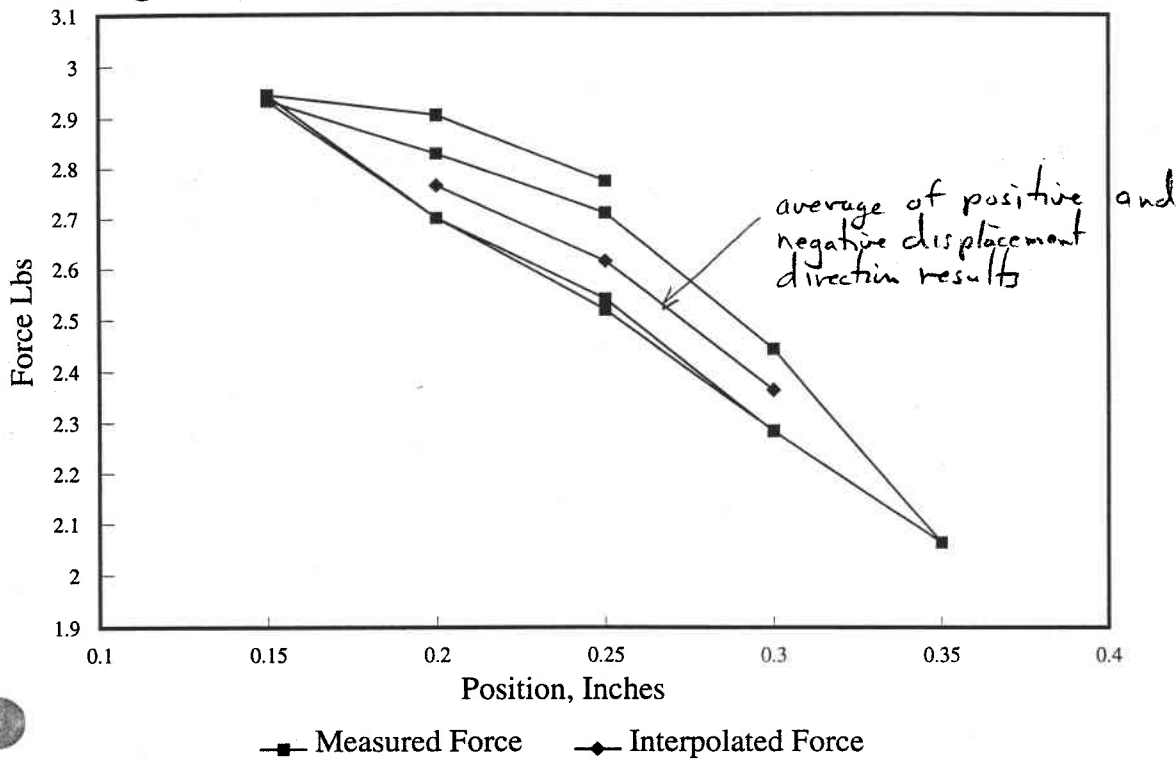


Figure B3 Stiffness Measurement



decreasing amplitude "shake-down" cycle at 0.25", 0.2", 0.15", 0.2" to 0.35", 0.3", 0.25" etc.

The resulting hysteresis at 0.25" amounts to about ± 0.045 lbs/support (fig. B3) but the hysteresis for ± 0.02 " motions from figure B2 is about 0.143 lbs/support. As used in the secondary mirror cell, the supports are displaced on startup by at most 0.08 inch and subsequently displace an amount equal to the elastic deflection of the secondary cell (about ± 0.005 "). Since in general all supports will be displaced equally on startup, startup hysteresis will tend to be equal for all supports. It is assumed that the variation in startup hysteresis will be 10% of that for 0.08" of motion. Extrapolation of the envelope of points in Figure B2 gives a value of 0.9 lbs for ± 0.04 inches of motion (0.45 lbs/support). 10% of this is 0.045 lbs/support.

The effect of cell deflection of ± 0.005 " was measured by examining the effect of ± 0.005 " steps on the test apparatus. The measured force change was ± 0.066 lbs allowing a minute for the force measurement to stabilize.

B.1.3 Stiffness Measurements

The stiffness of a support is determined from the data plotted in Figure A3. The maximum measured slope (stiffness) is 2.77 lbs/inch. Allowing 0.03" for installed height variations, the expected error force is $0.03 \times 2.77 = 0.083$ lbs.

Letting k be the diaphragm stiffness per unit circumference:

$$\begin{aligned} \text{Axial Stiffness} &= \pi Dk &&= 2.77 \text{ lb/inch so } k=0.69 \text{ lb/inch} \\ \text{Moment Stiffness} &= \pi D^3k/8 &&= 0.57 \text{ in-lb/radian} \end{aligned}$$

The moment stiffness is obtained as follows:

$$\begin{aligned} I &= \pi R^3t \\ f &= MR/(It) \text{ from which } M = ft/R = \pi fR^2 \\ \delta &= f/k \text{ and } \theta = \delta/R \text{ so } M/\theta = \pi R^3k = \pi D^3k/8 \end{aligned}$$

$$R = D/2$$

I = the moment of inertia of an annulus of thickness t and radius R

f = the maximum load per unit circumference

M = the net applied moment

δ = the maximum axial deflection at a point at radius R

θ = the rotation of the piston

B.2 Axial Support Error Forces

Results:

$$\begin{aligned}F_r = F_t &= 0.007 \cdot F_{ax} = 0.16 \text{ lbs max} \\M_r = M_t &= 0.372 \text{ in lbs} = 0.016 \cdot F_{ax} \\F_{ax} &= 23.2 \pm 0.14 \text{ lbs} \\M_z &= 0.4 \text{ in-lb}\end{aligned}$$

Axial Supports

The axial supports are defined by drawing #???????. These actuators are built around a Bellofram class 4 diaphragm 1.37 x 1.19 x 1.37 height, "C" sidewall thickness, and an .090" convolution and a similar diaphragm 1.25 x 1.06 x 1.25 and an 0.095" convolution (for supports in the outer row).

Effective pressure diameter, D , of the selected diaphragms = 1.28" and 1.155" .

Effective pressure areas are 1.28 in² and 1.04 in² resp. giving a force ratio of 1 : 0.813 .

The axial support system consists of 36 pneumatic supports in three zones and three hard points equipped with load cells with growth potential to add pzt position adjustment. The load cells limit axial force at each hard point to 0.25 lbs.

The axial support assemblies, Figure B.4, contain a Bellofram diaphragm and a wire connection from a point 1.5 to 1.75 inches below the diaphragm convolution to the mirror back connection which is at least 2.547 above the glass surface. Allowing 1.0 inch for interfaces leaves a minimum of 1.5 inches of wire from a point at least 1.45 inches below the diaphragm convolution to a point 0.86 inches (max) above the glass.

Axial Support design parameters:

- convolution to wire 1.5 to 1.75"
- free wire length = 1.5" min
- glass to free wire = 0.86" max
- positioning (relative) = ± 0.020 "

Special Considerations for Uniform Axial Force:

Adjust wire ends (interface to support) to be reference height
 ± 0.021 "

Allowance for diaphragm to diaphragm variation = 0.021"

Total effective height variance = $\text{SQRT}(.021^2 + .021^2) = 0.03$ "

Estimated axial force variation = 0.03 " * 2.77 lb/inch
= 0.083 lbs

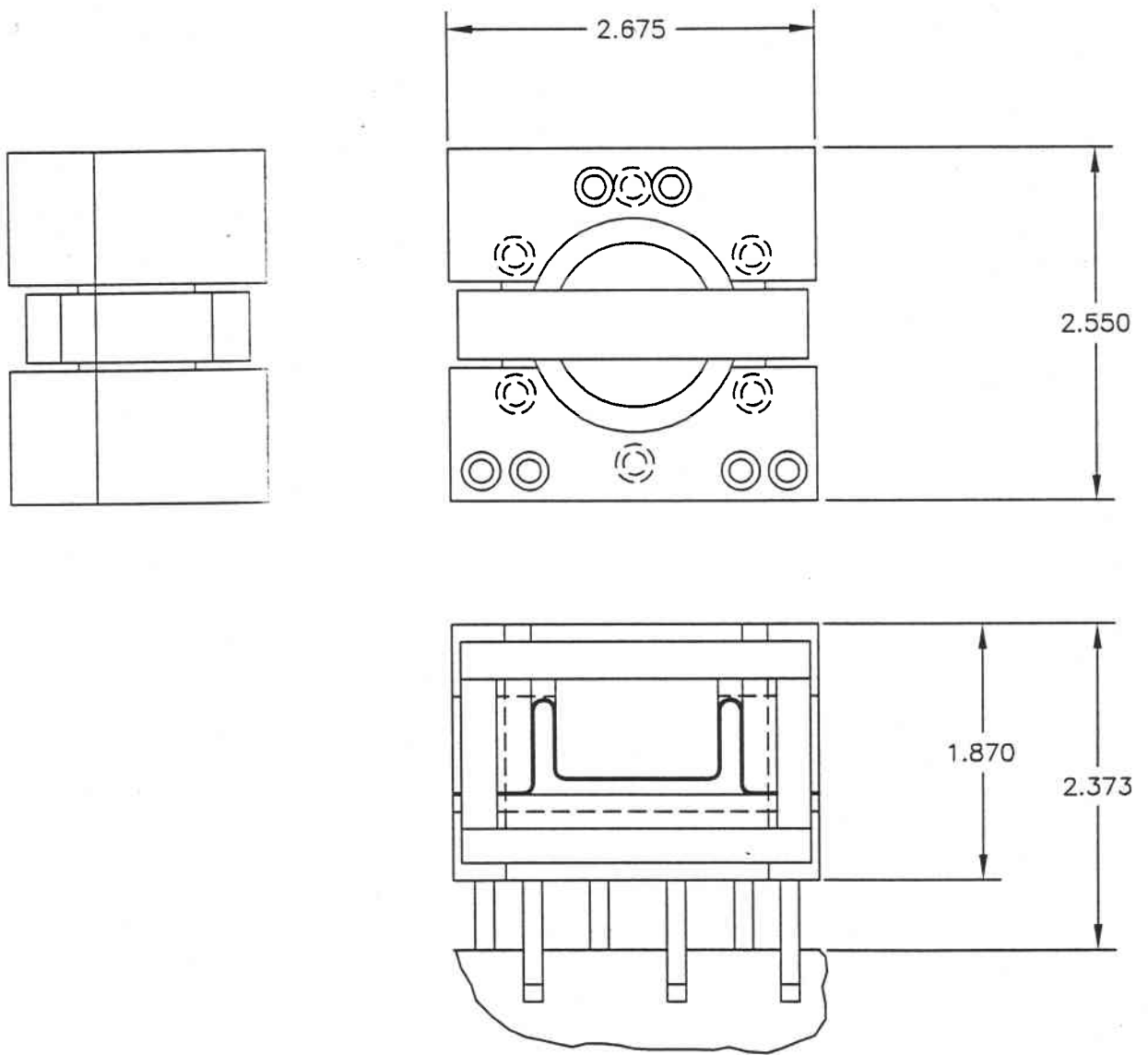


Figure ~~84~~ ⁰⁴

Axial Actuator Concept
 /home/bcuerden/mmt/f9sec/dwgs/
 axial-spt.dwg

9

B.2.1 Axial Force Error

The axial force error consists of the hysteresis forces (ref B.1.2) of 0.045 lbs and 0.066 lbs and a force related to the axial spring rate of the support and the uniformity with which the axial positions of the supports are placed. The procedure described above limits the installed axial force error to 0.083 lbs. The RSS of these values is 0.115 lbs. The design is based on an axial error force of 0.14 lbs.

B.2.2 Lateral Force Errors (Shears and Moments)

Position error effects (F_r , F_t , M_r , M_t)

The position error is accommodated by rotation of the actuator piston and deflection of the wire. This calculation considers a 2.6 in-lb/radian diaphragm (ref. B.1), a 1.5 inch offset to the top of the wire (L_d) and 1.5 inches of wire (L_w).

$$\begin{aligned}M_d &= L_d * V - F_{ax} * \delta_1 \\ \delta_1 &= L_d * M_d / K_\theta \\ V &= (\delta - \delta_1) * F_{ax} / L_w\end{aligned}$$

Where: M_d , K_θ = the diaphragm moment and stiffness,
 $K_\theta = 2.6$
 L_d = the distance from convolution to wire, 1.5" min.
 L_w = the free length of the wire, 1.5" min
 V = the shear force
 δ , δ_1 = the total deflection and the deflection at the top of the wire, $\delta = 0.02$
 F_{ax} = the axial force per support = 23.2 lb max

Combining equations gives:

$$V = \delta * (L_w / F_{ax} + L_d^2 / (K_\theta + L_d * F_{ax})) = 0.16 \text{ lbs} \quad (\approx 0.007 * F_{ax})$$

The moment referenced to the midplane of the back sheet is:

$$M_{\text{mid-plane}} = V * (0.86 + .256) = 0.18 \text{ in-lb.}$$

(.86" = the distance from the back of the mirror to the wire
.256" = half the thickness of the mirror back)

There is also a position error moment. Assuming the 0.020 relative error is split (RSS) between mirror and cell (.014" each), the position error moment is:

$$M_{pos} = .014 * F_{ax} = .325 \text{ in-lb}$$

The RSS net moment is:

$$\begin{aligned} M_r = M_t &= \text{sort}(0.18^2 + 0.325^2) = 0.372 \text{ in-lb} \\ &= 0.016 * F_{ax} \end{aligned}$$

B.2.3 Torsion (Mz)

Assuming 0.060" wire with a strand angle of 20 degrees. The torsion is estimated as:

$$\begin{aligned} M_z &= 0.4 * D_{\text{wire}} * \sin(20) * F_{ax} = .19 \text{ in-lb} \\ \text{This is doubled for design, } M_z &= 0.4 \text{ in-lb} \end{aligned}$$

B.3 Axial Locator Force Errors

$$\begin{aligned} F_r = F_t &= 0.19 \text{ lbs} \\ M_r = M_t &= 0.90 \text{ in-lbs} \\ F_{ax} &= 0.25 \text{ lbs} \\ M_z &= 1 \text{ in-lb} \end{aligned}$$

B.3.1 Flex rod:

Distance between extreme flexures = 5"
 Midplane of back to middle of nearest flexure = 1.0"
 Flexures: .25 wide by 0.04 thick by 0.5 inches long. 0.03 radii at ends
 Rod: 0.25 dia., 0.25" of rod between flexures (steel, E=28e6)
 Installation (relative) 0.01" and 0.25 degrees
 Maximum axial force = 0.25 lbs

Flexrod input: 7,1,1.75,.25,.04,.43,28e6,.01,.25,.25 (f9flex.in)

Results:

$$\begin{aligned} 1/5 F_{crit} &= 398 \text{ lbs (max allowable axial load)} \\ \text{Flexure stress at } 0.25 \text{ lbs} &= 13,525 \text{ psi} \\ \text{Flexure stress at } 1g &= 24,781 \text{ psi} \\ V &= 0.19 \text{ lbs} \\ M &= 0.90 \text{ in-lbs} \end{aligned}$$

B.3.2 Axial Force Error and Torsion

The axial error force is limited by the load cell to 0.25 lbs.

Torsion must be limited to 1 in-lb by careful assembly.

B.4 Lateral Support System, Pneumatic Lever Arm Supports

Support characteristics (ref Figure B.5)

Lever Arm

Lever arm mechanical advantage:	1:1 matched to 0.01"
Lever arm length :	greater than 3"
Lever arm pivot bearing:	.5" Dia anti-friction ($\mu = 0.005$)
Lever arm balance:	imbalance < 0.4 in-lbs

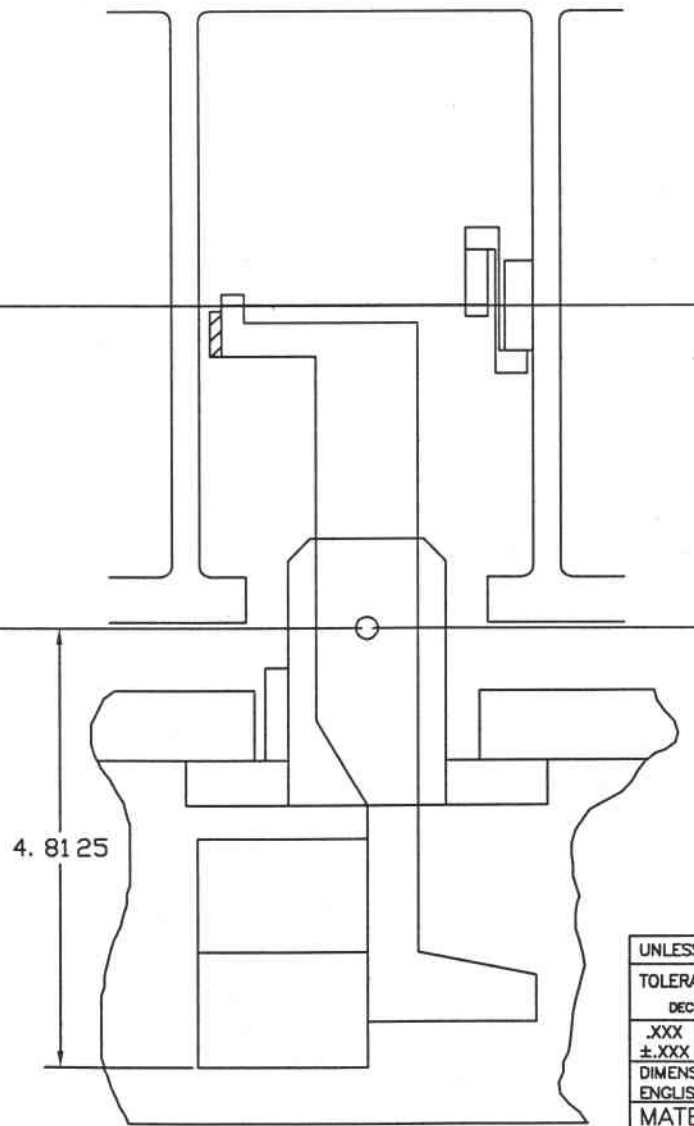
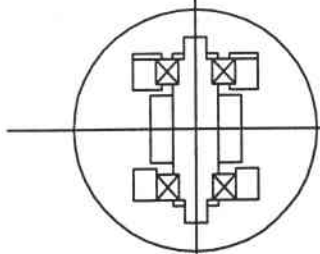
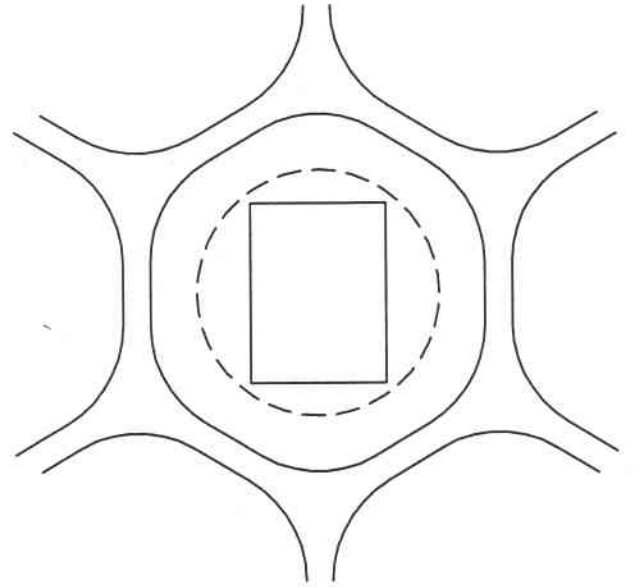
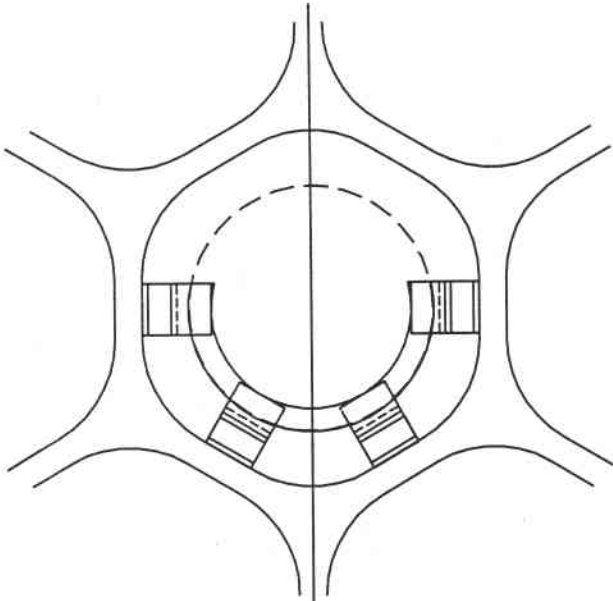
Connecting Link

Length:	more then 2.0"
Parallel to back plate:	0.008"
Link tolerance contribution	0.008"
Pivot bearing (each end)	$\mu = 0.2$ Pin Dia = 0.19
Flexure (free section)	.625x.010x2"

Performance, Net:

$$\begin{aligned}F_x &= 0.559 & = 0.559 \sin(\theta) \\F_y &= 0.152 & = 0.1268 + 0.028 \sin(\theta) \\F_z &= 0.148 & = 0.043 + 0.1044 \sin(\theta) \\M_x &= 0.057 \\M_y &= 0.056 \\M_z &= 0.50 & = 0.5 \sin(\theta)\end{aligned}$$

The lateral support system consists of 30 pneumatic supports in two rows of 6 and 24 and three tangent rods. The pneumatic supports, Figure B.2, act in the N/S direction with all forces being applied at the CG plane or up to 0.050" toward the back of the secondary from the CG plane. Supports consist of a rolling diaphragm pneumatic cylinder acting on a balanced lever that transfers the load to the cg plane. The connection to the mirror is by a thin strip of stainless steel, reinforced at the ends for a



ES:

X REQUIRED.

SEE DWG. #XXXX FOR PLACEMENT.

FIGURE B5
LATERAL Actuator

(ref: /home/buenden/mmt/fssec/telcell/drgs/laterals.dwg)

UNLESS OTHERWISE SPECIFIED
TOLERANCES
DECIMALS
.XXX
±.XXX
DIMENSIONS
ENGLISH
MATERIAL
FINISH

pin connection. Lateral forces must act parallel to the backplate to within 0.14 degrees (8.5 minutes or 2.5 m-rad).

B.4.1 Connecting Link, $F_x = 0.559$ lbs, $F_z = 0.148$
 $M_x = 0.057$ in-lbs, $M_y = 0.056$ in-lbs, $M_z = 0.5$

Pin Friction Loads:

$$\text{Dia} = 0.19, \quad \mu = 0.2, \quad F = 25 \text{ lbs/spt}$$

$$M = 0.2 * 0.5 * .19 * 25 = 0.475 \text{ in-lb}$$

Axial location of link ends is 1 lb (wave spring of 0.25 OD) on teflon washers:

$$M = 2 * (0.5 * .25 * .1 * 1) = 0.025 \text{ in-lb}$$

Net friction moment, $M_z = 0.5$ in-lb

Shear reaction, $F_x = 2 * .5 / 2 = 0.5$ lbs

Alignment:

Z alignment errors: 0.008" installation error, 0.008" fabrication error

$$F_z = 0.0113 * 25 / 2" = 0.141 \text{ lbs}$$

X alignment error: 0.020"

$$F_x = 0.020 * 25 / 2" = 0.25 \text{ lbs}$$

End pitch and tilt:

Link twist of 2 degrees per end (= $1.414 * 0.035 = 0.05$ rad):

$$M_y = 0.05 * G * t^3 * \text{width} / (3 * L) = 0.056$$

t, width, L = link thickness, width and length
 = 0.010", 0.625" and 2"

G = shear modulus (10.76E6)

Link end pitch of 1 deg/end: (Ref. Roark, IV ed. III.29)

$$\theta = 0.25 * ML / EI \quad F_y = 1.5 * M / L$$

$$M = 2.92\theta = 0.051 \text{ in-lb}$$

M from tilt at opposite end = 0.0255 in-lb

M_x net = 0.057 in-lb

F_z = 0.043 lbs

B.4.2 Lever Arm and Pneumatic Cylinder, $F_y = 0.152$ lbs

Lever arm pivot friction:

Moment = $0.5 * 0.5 * 0.005 * 50$ lbs = 0.0625 in-lb

F_y error = 0.0625 lbs/3 inches = 0.021 lbs

Lever arm length tolerance of 0.010"

$F_y = (3.01/3-1) * 25 = 0.0833$ lbs

Pneumatic Cylinder (0.125 lbs force error used for design, 0.10 lbs predicted)

Stiffness Effects:

Install to within 0.021" of nominal stroke at nominal position.

Allowance for sample to sample height variation = 0.021" .

Net height variation = 0.030"

Using the stiffness of 2.77 lb/inch (ref. B.1.3)

F_y stiffness = 2.77 lb/in * 0.030 " = 0.083 lbs

Hysteresis Effects:

Startup height change of 0.080" maximum:

$F_y = 0.045$ lbs (ref. B.1.2)

Cell deflections (less than ± 0.0025 " lateral support height change)

$F_y = 0.033$ lbs (half the value in section B.1.2 for 0.005" deflection).

Net hysteresis $F_y = 0.056$ lbs

Net cylinder error force predicted = 0.10 lbs (Use 0.125 lbs for design).

B.5 Lateral Locator Force Errors (Tangent Rods)

$$\begin{aligned}F_r &= F_z = 0.19 \text{ lbs} \\M_r &= M_z = 0.90 \text{ in-lbs} \\F_t &= 0.25 \text{ lbs} \\M_t &= 1 \text{ in-lb}\end{aligned}$$

B.5.1 Flex rod:

Distance between extreme flexures = 5"
Center of rod to middle of nearest flexure = 1.0"
Flexures: .25 wide by 0.04 thick by 0.5 inches long. 0.03 radii at ends
Rod: 0.25 dia., 0.25" of rod between flexures (steel, $E=28e6$)
Installation (relative) 0.01" and 0.25 degrees
Maximum axial force = 0.25 lbs

Flexrod input: 7,1,1.75,.25,.04,.43,28e6,.01,.25,.25 (f9flex.in)

Results:

$$\begin{aligned}1/5 F_{crit} &= 398 \text{ lbs (max allowable axial load)} \\ \text{Flexure stress at } 0.25 \text{ lbs} &= 13,525 \text{ psi} \\ \text{Flexure stress at } 1g &= 24,781 \text{ psi} \\ V &= 0.19 \text{ lbs} \\ M &= 0.90 \text{ in-lbs}\end{aligned}$$

B.5.2 Axial Force Error and Torsion

The axial error force is limited by the load cell to 0.25 lbs.

Torsion must be limited to 1 in-lb by careful assembly.

B.6 Location of Lateral Support Plane Relative to CG

The Lateral Supports are nominally applied in the CG plane. The accuracy with which the support plane must be established is considered in this section. In Table B.6.1, results for different support plane locations are compared.

Table B.6.1 Comparison of Different Support Plane Locations

Tabulated Values are the maximum value (in millionths of an inch) of the structure function (typically at or near the maximum distance)
 Lateral Support is 24 near the OD and 6 at 70% near the center

	Support Plane Relative to CG, + is Toward Face		
	+ .020"	0.00	-0.05"
1g X	1.148	1.095	1.580
Zen. to 30	0.679	0.568	0.633
Zen. to 45	1.155	0.908	0.892
Zen. to 60	1.699	1.310	1.196
Zen. to Horiz.	2.855	2.382	1.896

The Zenith to 60 degree combined structure function was computed with the cg at the extremes indicated in Table B.6.1 . Results indicate that the support plane must lie between the cg plane and 0.050" behind (toward the secondary back plate) the cg plane.

B.7 Astigmatism

Astigmatism is the softest deformation mode of the mirror. Error force distributions that could generate astigmatic deformations must be identified and accounted for. Two sources of astigmatic distortion are considered here, cell bending and random chance.

B.7.1 Randomly Generated Astigmatic Force Distributions

When the 36 axial supports are installed, the axial error force of each support is estimated to be 0.115 lbs (see B.2.1). By random chance, the error forces will occasionally include a $\sin(2\theta)$ component. The magnitude of this component was established using a Basic program to generate multiple sets of random numbers from which the $\sin(2\theta)$ component was extracted. By using 1000 or more sets of 36 values, the mean coefficient of the $\sin(2\theta)$ term was driven close to zero, but the standard deviation of the values of the coefficient was 0.135 (for force errors between -1 and +1). For future reference, the standard deviation for the random astigmatic coefficient was compiled for different numbers of supports with the results included in Table B.7.1 .

We want to obtain an estimate for the randomly introduced astigmatism that we won't exceed more than 10% of the time so we need to design to a random astigmatic coefficient that is 1.65 times the standard deviation. Since there are sine and cosine astigmatic terms, the design value for random astigmatism becomes $1.65\sqrt{2}\sigma$ (σ = the standard deviation). These design values are listed in Table B.7.1 for unit (\pm) error forces.

Table B.7.1 Normalized Coefficients for Random Astigmatic Force Distributions

# of Forces	# Data Sets	Mean Coef	σ	Design Coef./F
6	1000	-0.004	0.345	0.805
8	1000	-0.0003	0.298	0.695
12	2000	0.0005	0.236	0.551
18	2000	-0.0063	0.189	0.441
24	1000	0.0045	0.167	0.390
36	2000	0.0023	0.135	0.315
54	1000	.0006	0.105	0.245

B.7.2 Astigmatic Forces Generated by Cell Sag

Static analysis of the f5 telescope cell gives astigmatic deflection coefficients of 0.000518 at zenith and 0.00213 at the horizon. Taking the net cell sag to be the sum of twice the axial plus the lateral (assumes face up alignment of the axial supports) gives a deflection of ± 0.0032 ". Acting through the axial actuator stiffness of 2.77 lb/in (ref B.1.3) this amounts to an astigmatic force coefficient of 0.009 lbs. The laterals respond to the 0.0032" deflection as $(0.0032/2.0) * 25 \text{ lbs} = 0.04 \text{ lbs}$.

Hysteresis forces for the ± 0.0032 " astigmatic deflection is 64% of that for 0.005" reported in section B.1.2 or 0.042 lbs. Combining this with the stiffness effect of 0.009 lbs gives 0.043 lbs.

Cell plate deflection summary:

Term	Units	Value	
		1g X	1g Zenith
Rotx	μ -rad	1310	367
Roty	μ -rad	30	2
P-V	milli-Inches	4.174	7.040
Zerneke Coefficients			
Sin Astigmatism	milli-Inches	0.038	0.002
Cos Astigmatism	milli-Inches	2.13	0.518
Power	milli-Inches	0.012	-0.471
Spherical	milli-Inches	0.003	-0.049

Cell deflection will effect lateral and axial supports simultaneously. Lateral and axial print-through forces are added and applied to the axial astigmatic force result.

Axials:

Cell print-through astigmatic force	= 0.043 lbs
Random force (36 spts ... $0.315 \cdot 0.115$)	= 0.036

Laterals:

Cell print-through astigmatic force	= 0.04 lbs
Random force (30 spts ... $0.353 \cdot 0.15$)	= 0.053

Loading Applied to Model:

Add print-through forces and apply to axials:	0.083 lbs
Axial random astigmatic force (max)	0.036 lbs
Laterals random force (max)	0.053 lbs

Appendix C Net Performance Tables

Table C1 F5 Secondary Surface Performance Zenith Pointing

Waves are 0.632 μ -m
See Addendum 1 for error force estimates and backup data

Load Case	Rms Surf Distortion		Max Slope arc-sec rms
	μ -inch	WF, λ	
Gravity, Zenith to Indicated Elev	0	0	0
Lateral and Axials Fz Astig. Cell Bend	0.284	0.0228	0.006
Axials Fz Astig, random	0.164	0.0132	0.004
Laterals Fz Astig, random	0.214	0.0172	0.005
Random Force Errors	1.026	0.0824	0.0216
RSS Total =	1.0982	0.0882	0.0233

Table C2 F5 Secondary Surface Performance 30 Degrees From Zenith

Waves are 0.632 μ -m
See Addendum 1 for error force estimates and backup data

Load Case	Rms Surf Distortion		Max Slope arc-sec rms
	μ -inch	WF, λ	
Gravity, Zenith to Indicated Elev	0.228	0.0183	0.0165
Lateral and Axials Fz Astig. Cell Bend	0.284	0.0228	0.006
Axials Fz Astig, random	0.164	0.0132	0.004
Laterals Fz Astig, random	0.214	0.0172	0.005
Random Force Errors	1.026	0.0824	0.0216
RSS Total =	1.1216	0.0901	0.0286

Table C3 F5 Secondary Surface Performance 45 Degrees From Zenith

Waves are 0.632 μ -m
 See Addendum 1 for error force estimates and backup data

Load Case	Rms Surf Distortion		Max Slope arc-sec rms
	μ -inch	WF, λ	
Gravity, Zenith to Indicated Elev	0.309	0.0248	0.0262
Lateral and Axials Fz Astig. Cell Bend	0.284	0.0228	0.006
Axials Fz Astig, random	0.164	0.0132	0.004
Laterals Fz Astig, random	0.214	0.0172	0.005
Random Force Errors	1.026	0.0824	0.0216
RSS Total =	1.1408	0.0916	0.0351

Table C4 F5 Secondary Surface Performance 60 Degrees From Zenith

Waves are 0.632 μ -m
 See Addendum 1 for error force estimates and backup data

Load Case	Rms Surf Distortion		Max Slope arc-sec rms
	μ -inch	WF, λ	
Gravity, Zenith to Indicated Elev	0	0	0
Lateral and Axials Fz Astig. Cell Bend	0.284	0.0228	0.006
Axials Fz Astig, random	0.164	0.0132	0.004
Laterals Fz Astig, random	0.214	0.0172	0.005
Random Force Errors	1.026	0.0824	0.0216
RSS Total =	1.0982	0.0882	0.0233

APPENDIX D Breakdown of Contributions to Net Mounting Error

This Appendix contains structure function plots which include selected sets of contributing factors. Similar plots were used to determine which design parameters had to be tightened to obtain acceptable performance. These plots may prove useful during the detail design and checkout phases.

The following lists define the specific content of the plotted curves. Unless otherwise noted, the curve can be regenerated by running `/home/bcuerden/programs/comb` which will ask for a jobname which is the name of the `.in` file. Output is written to the `jobname.spd` file which can be loaded into works to be plotted and to the `jobname.prt` file which includes a line printer plot. The files used to generate the plots in this Appendix currently reside in `/home/bcuerden/mmt/f5sec/comb`. The files which generate the net performance plots at zenith, 30 45 and 60 degrees from zenith are the `telz.in`, `tel30.in`, `tel45.in` and `tel60.in` files.

Plot D1 Zenith Pointing

BC1	This consists of the three astigmatic force sets (ref. B.7.2)
BC2	The contribution of the 36 axial supports less the axial force components.
BC4	The contribution of the three fixed axial locators.
Allowable	This is the Zenith Pointing allowable.

Plot D2 Zenith Pointing

BC3	The contribution of the 36 axial support axial force components.
BC5	The contribution of the lateral and tangent supports less the Fz components.
BC6	The contribution of the lateral and tangent support axial force components.
Allowable	This is the Zenith Pointing allowable.

Plot D3 Gravity Sag

Zenith Gravity	This is the gravity deflection when zenith pointing. Note that the mirror is figured in this orientation so this deformation is polished out.
Horizon gravity	The theoretical deformation due to lateral gravity.
Zenith to Horizon	This is the change in mirror figure in rotating from zenith to the horizon.
Allowable	This is the Zenith Pointing allowable.

Figure D1 Structure Function Components
Zenith Pointing Error Sources

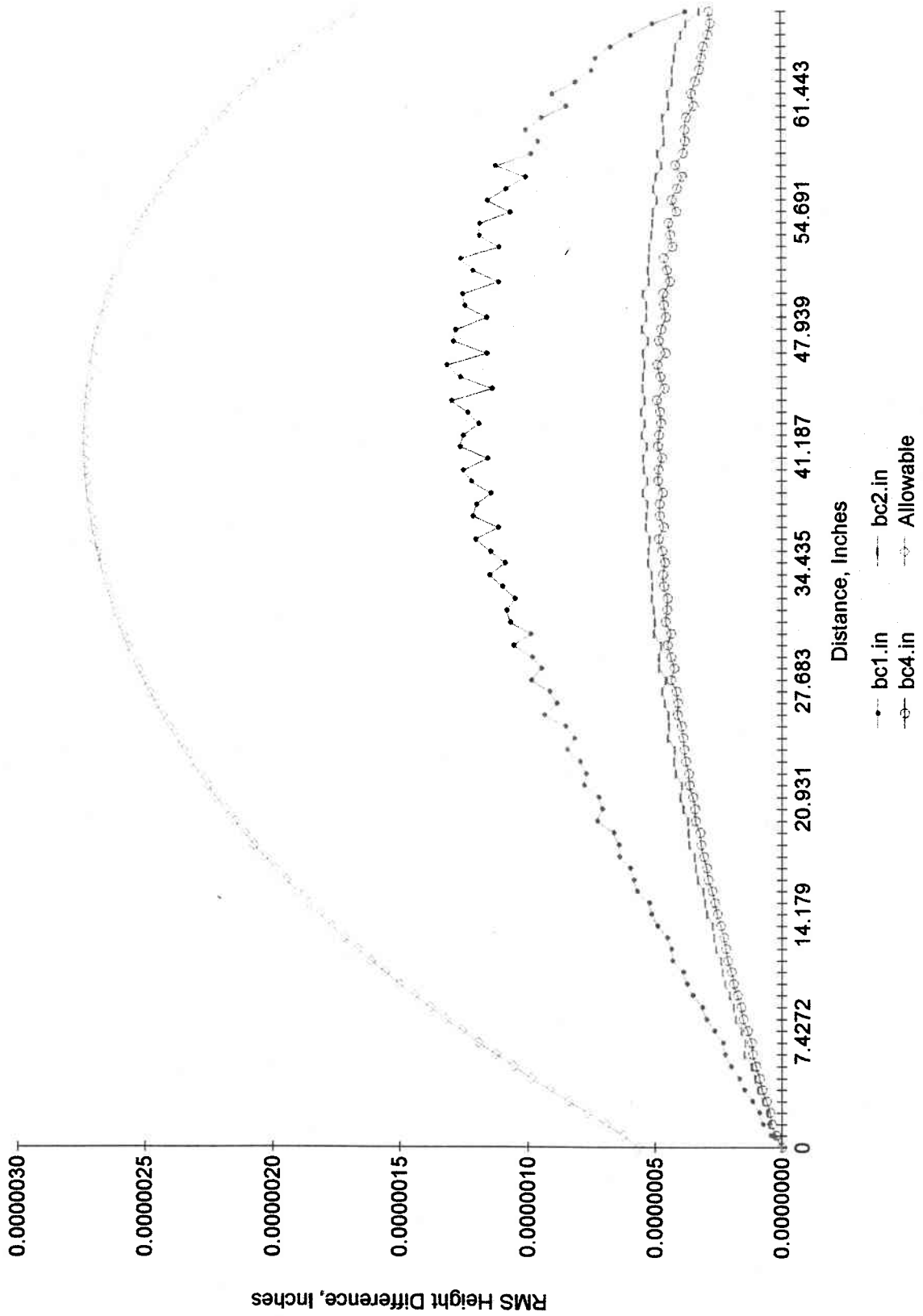


Figure D2 Structure Function Components
Zenith Pointing Error Sources

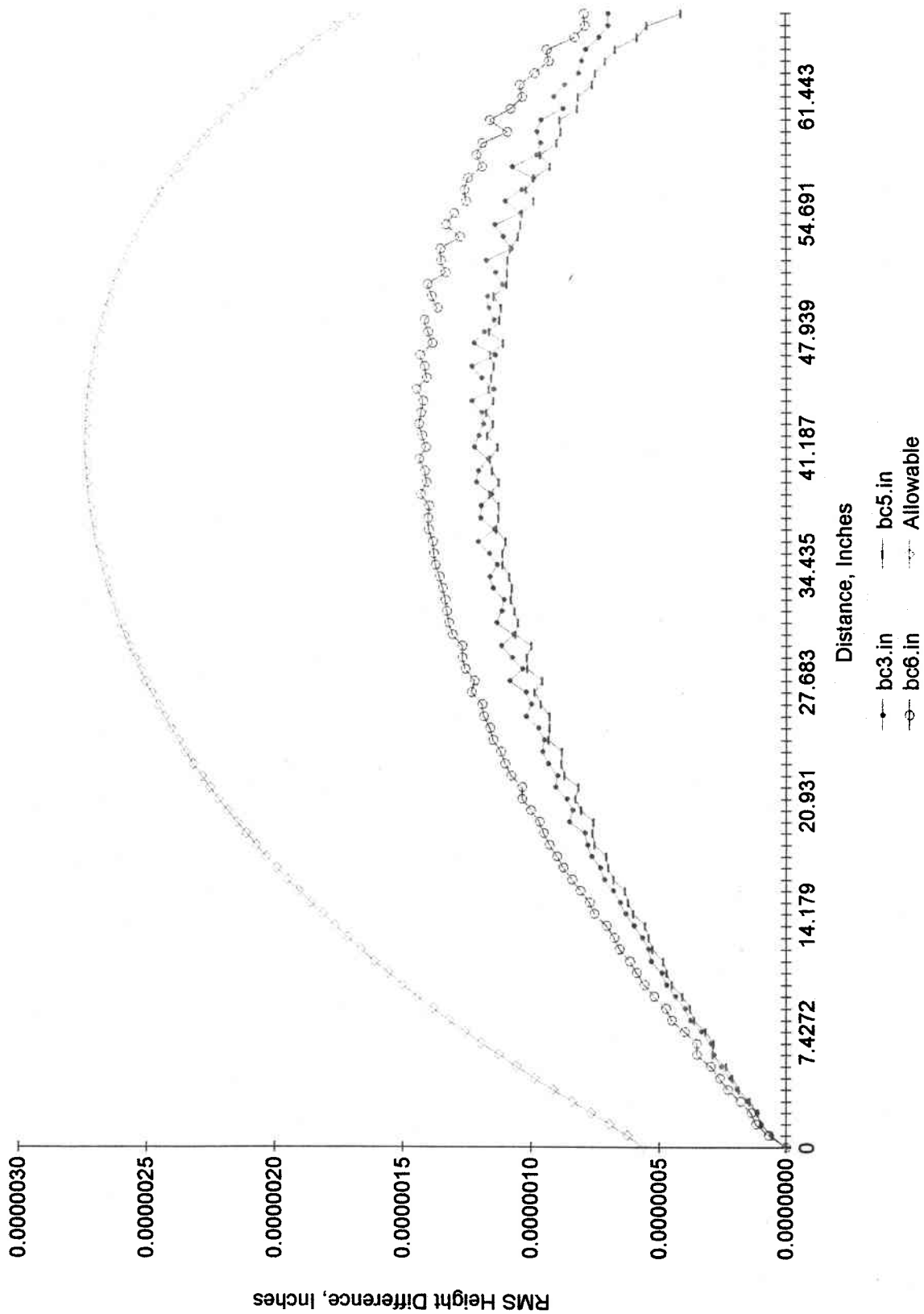
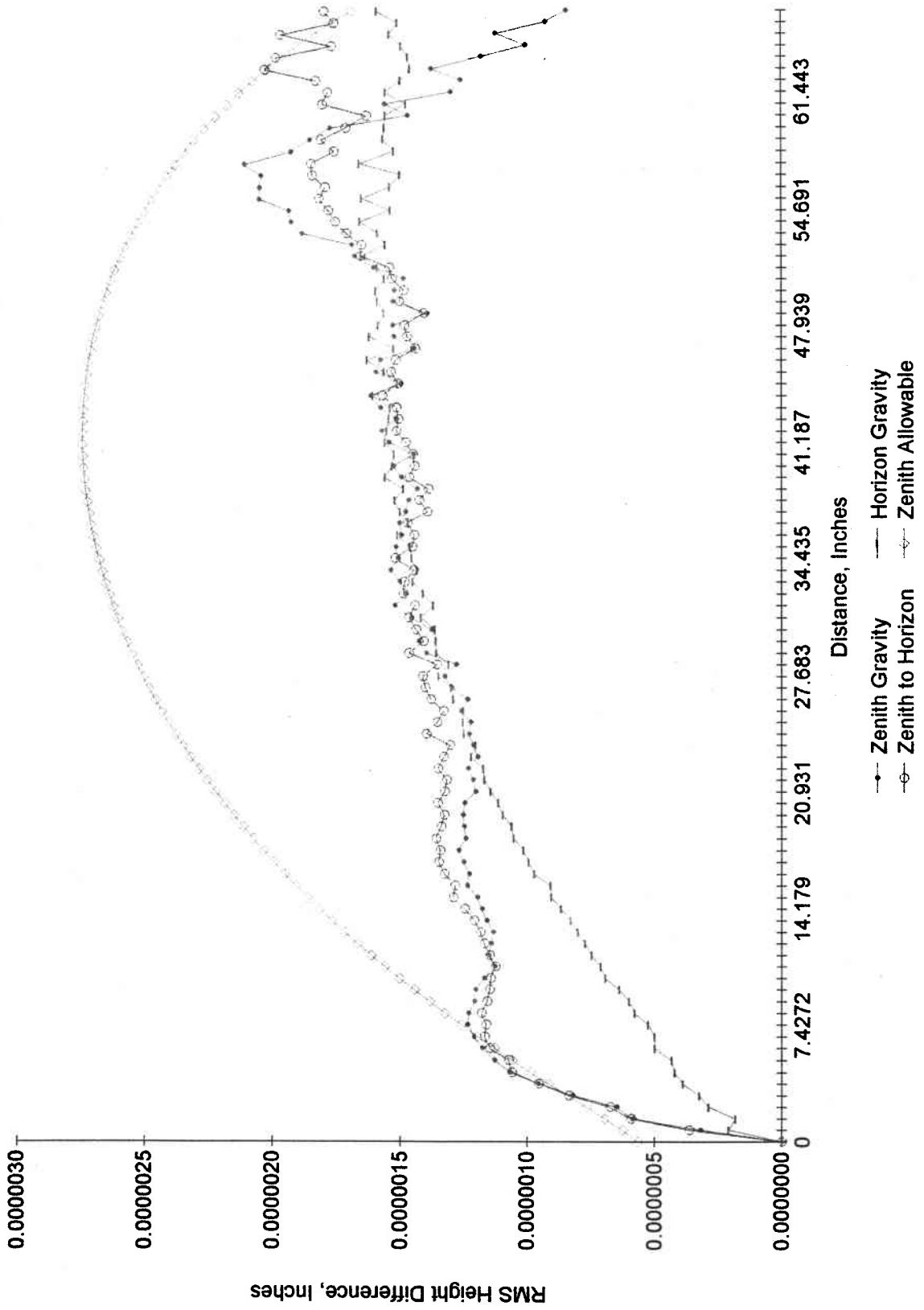


Figure D3 Structure Function Components
Gravity Sag Effects



Appendix E Notes on Generating Net Structure Function Plots

Generating the structure function plots used in this report was a four step process. Intermediate files have been saved to enable revised plots (different error force levels) to be generated with relative ease.

The complete process starts with several ANSYS runs to develop the surface distortion results for various load cases. The program slps is then run to remove translation tilt and power from the ANSYS surface normal displacement results and to generate a file containing the structure function for each load case. Each structure function consists of 100 sets of distance, height difference values. Structure functions are saved to a filename.stf file which have been preserved.

To generate a structure function which is a combination of several available load cases, one simply runs comb. Input parameters to comb contain the definition of the allowable structure function and the names of the files containing the load cases, the load case number of the desired case in a given file, and the scale factor for the load case. Comb combines the specified load cases and generates a crude printer plot and a tabular listing of the result. It also writes a filename.spd file which can be loaded into a works spreadsheet for plotting.

All f5 secondary .stf files are in /home/bcuerden/mmt/f5sec/comb . Numerous sample input files (filename.in) are included.

APPENDIX F Cell Configuration

The cell configuration is shown in Figure F.1 . The lateral and axial support concepts are shown in Figures F.2 and F.3 . The cell structure is aluminum for reduced weight. Thicknesses and all up cell weight are listed below.

Item	Thickness
Cell Webs (4 inches deep)	0.5"
Cell Disk	0.75"

Weight (including mirror) = 1350 lbs

Inertias:

$$I_{xx} = I_{yy} = 950 \text{ in-lb-sec}^2$$

$$I_{zz} = 1900 \text{ in-lb-sec}^2$$

CG = 0,0,-7.37 (z=0 is the hexapod interface plane)

ref phone/bureau rdan/mmt/f/5 scan the cell layout of tel-cell.dwg

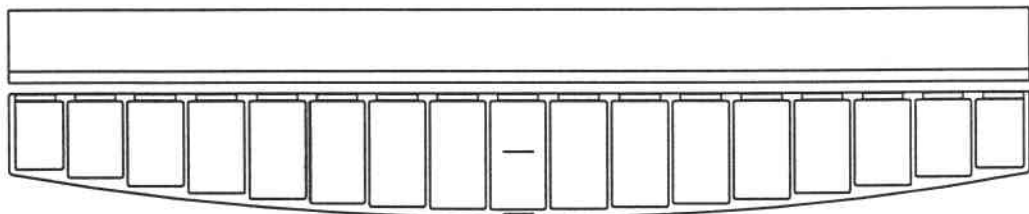
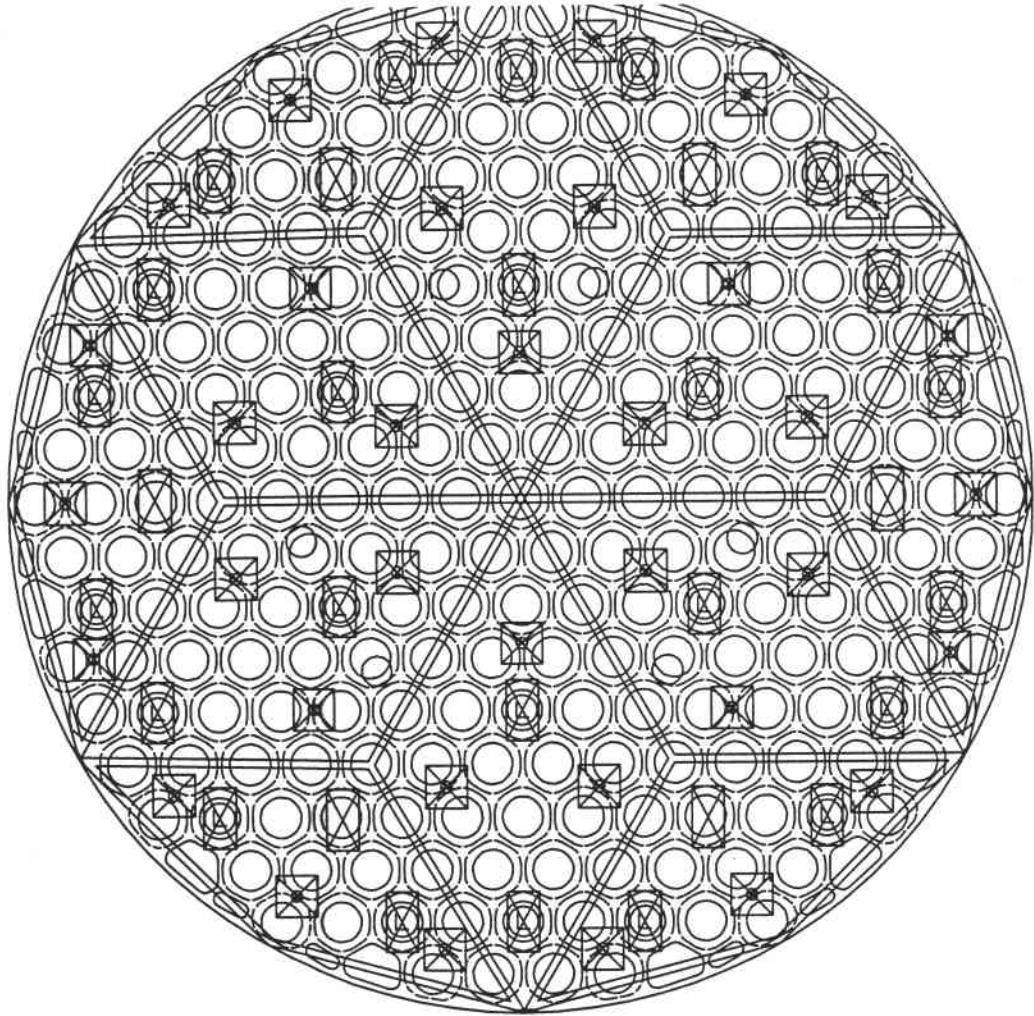
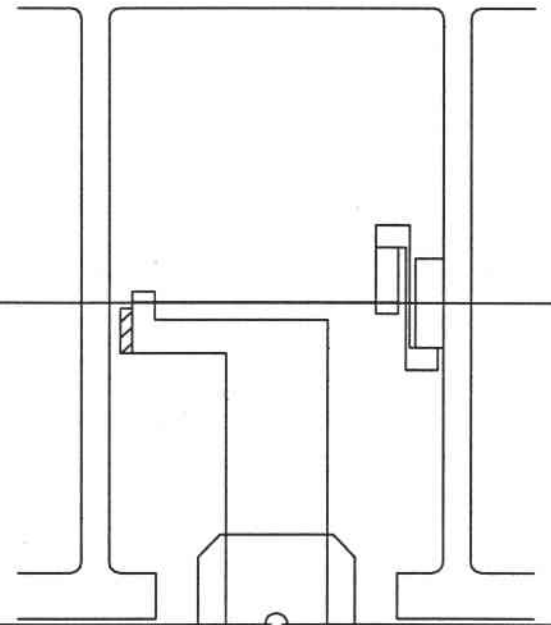
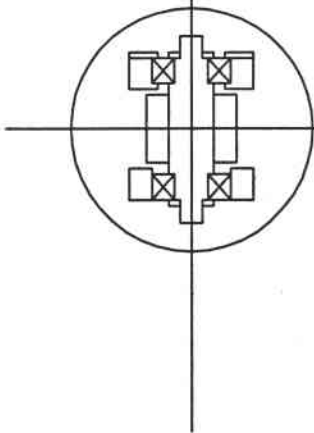
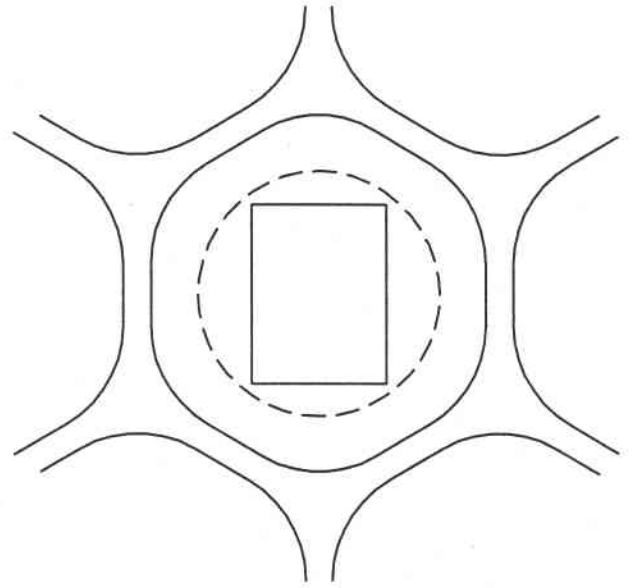
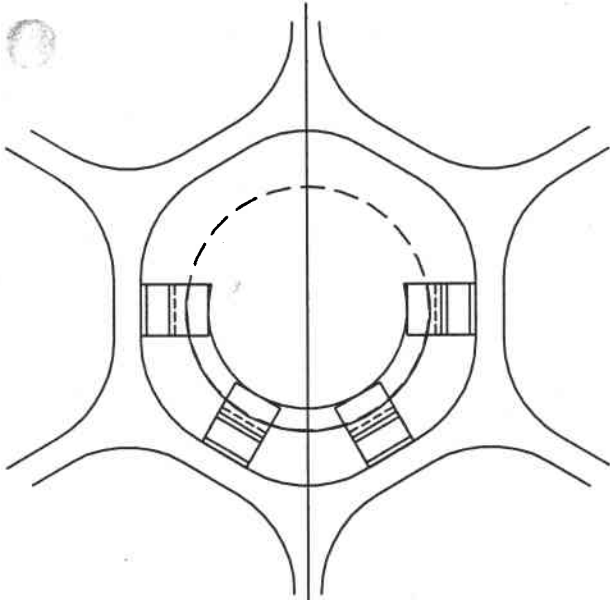


Figure F1 MMT f/5 Cell Layout



4.8125

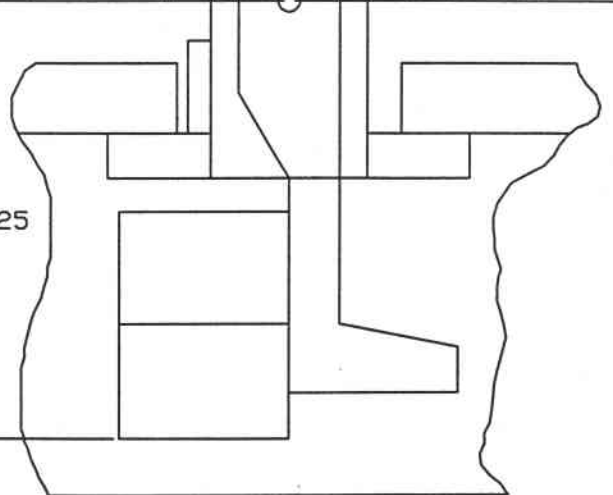


Figure F2 Lateral Support (\\home\b cuerden\mmt\f5sec\ tel cell \dwgs\lateral s. dwg

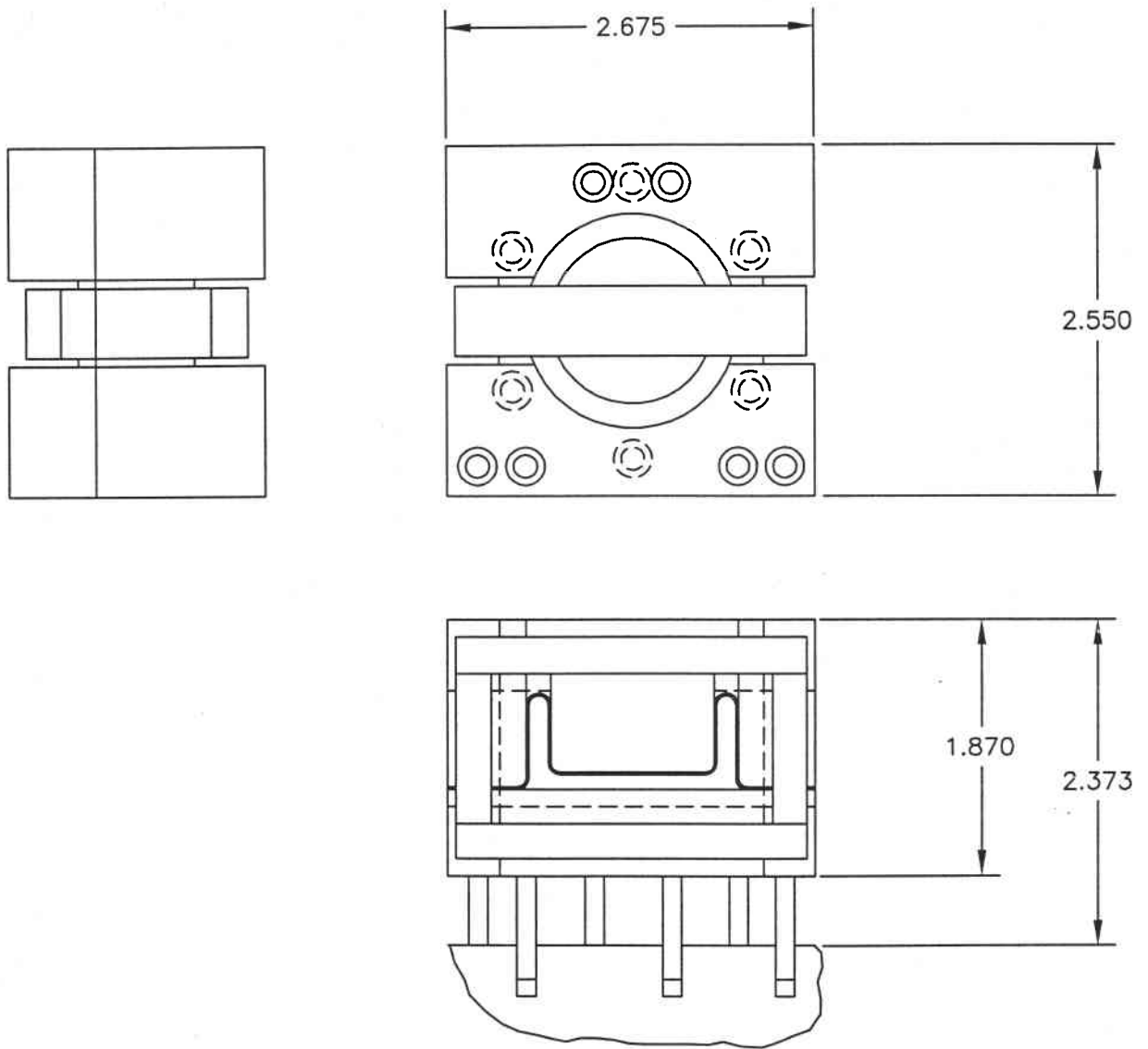


Figure F.3 Axial Actuator Concept
 /home/bcuerden/mmt/f9sec/dwgs/
 axial-spt.dwg

APPENDIX G Wind Loading Effects

References:

1. My memo to S. West dated: 24-May-97, Subject: Wind Distortion of the MMT Primary and f/9 Secondary Mirrors
2. West, S. C. and Martin, H. M. "Approximate Wind Disturbance of the MMT 6.5 M Mirror on its Supports". MMT technical Report # 28.

Reference 2 defines a method of calculating the dynamic wind force acting on the mirror and reacted by the fixed support points. In reference 1, the distortions resulting from these support point reactions were calculated for the primary mirror and the f/9 secondary. This same procedure has been used to obtain wind induced reaction forces and the resulting distortion for the f/5 secondary. The reaction forces for various bandwidths of the control system (fixed point force to pneumatic pressure loop) are listed in Table G.1 .

Table g.1 Fixed Point Reactions Verses Wind Speed and Control System Bandwidth

Control System Bandwidth	Net Reaction Force, Lbs					
	No Control No De-correlation		Control No De-correlation		Control And De-correlation	
Wind V =	6.7 m/sec	22 m/sec	6.7 m/sec	22 m/sec	6.7 m/sec	22 m/sec
1 Hz	1.02	15.7	0.399	6.357	0.234	4.898
3 Hz	1.02	15.7	0.277	4.418	0.107	2.697
4 Hz	1.02	15.7	0.251	4.004	0.084	2.234
5 Hz	1.02	15.7	0.233	3.714	0.070	1.916
6 Hz	1.02	15.7	0.219	3.495	0.059	1.682

The 3 Hz bandwidth forces with no decorrelation were applied to the f/5 secondary model resulting in the structure function shown in Figure G1 for fixed axial supports located on a 26" radius circle. The structure function for fixed axial supports located on a 30" radius circle is shown in Figure G2.

Figure G1 Structure Function, MMT f/5
 Wind Loading, Spts @26" Radius

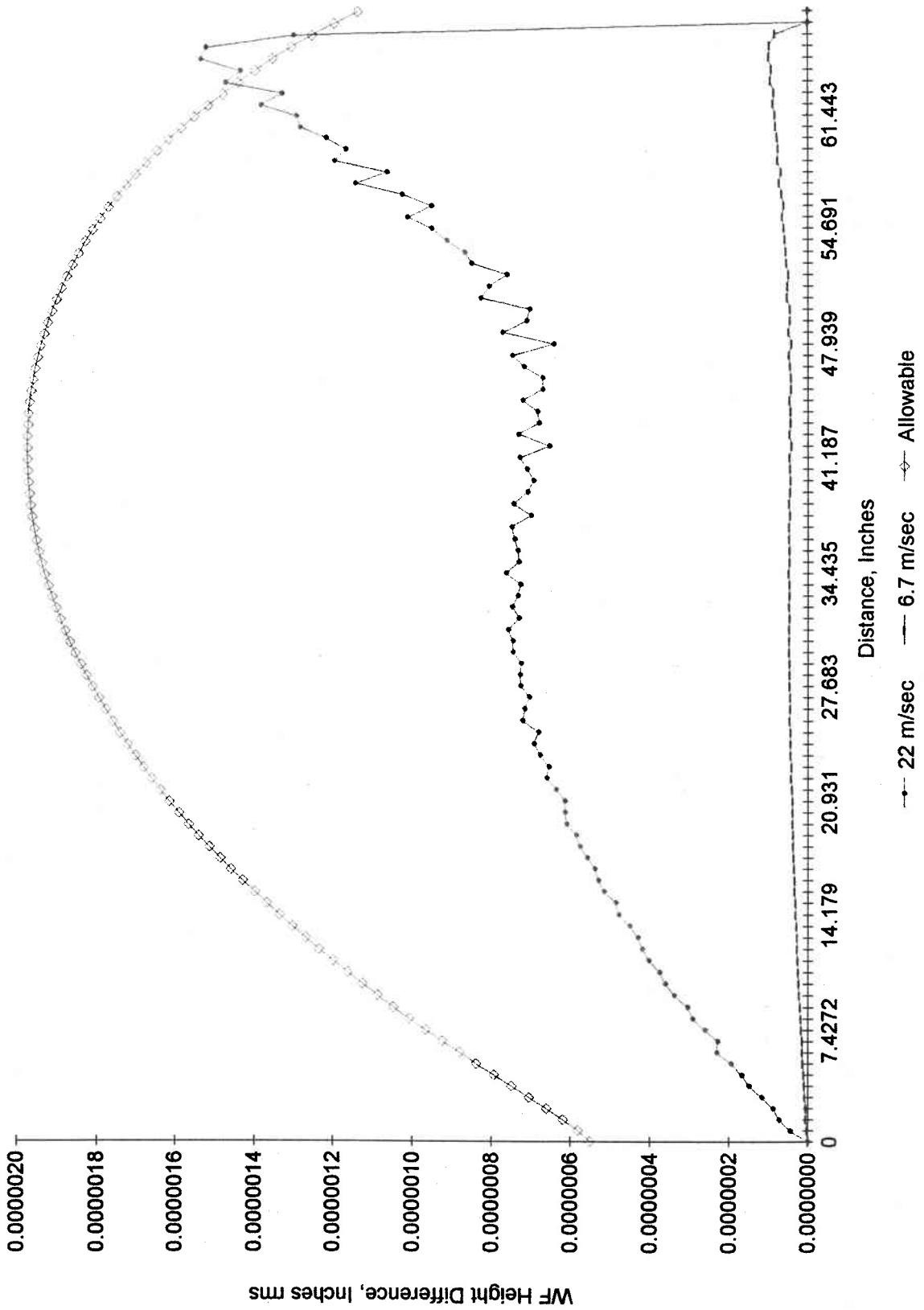
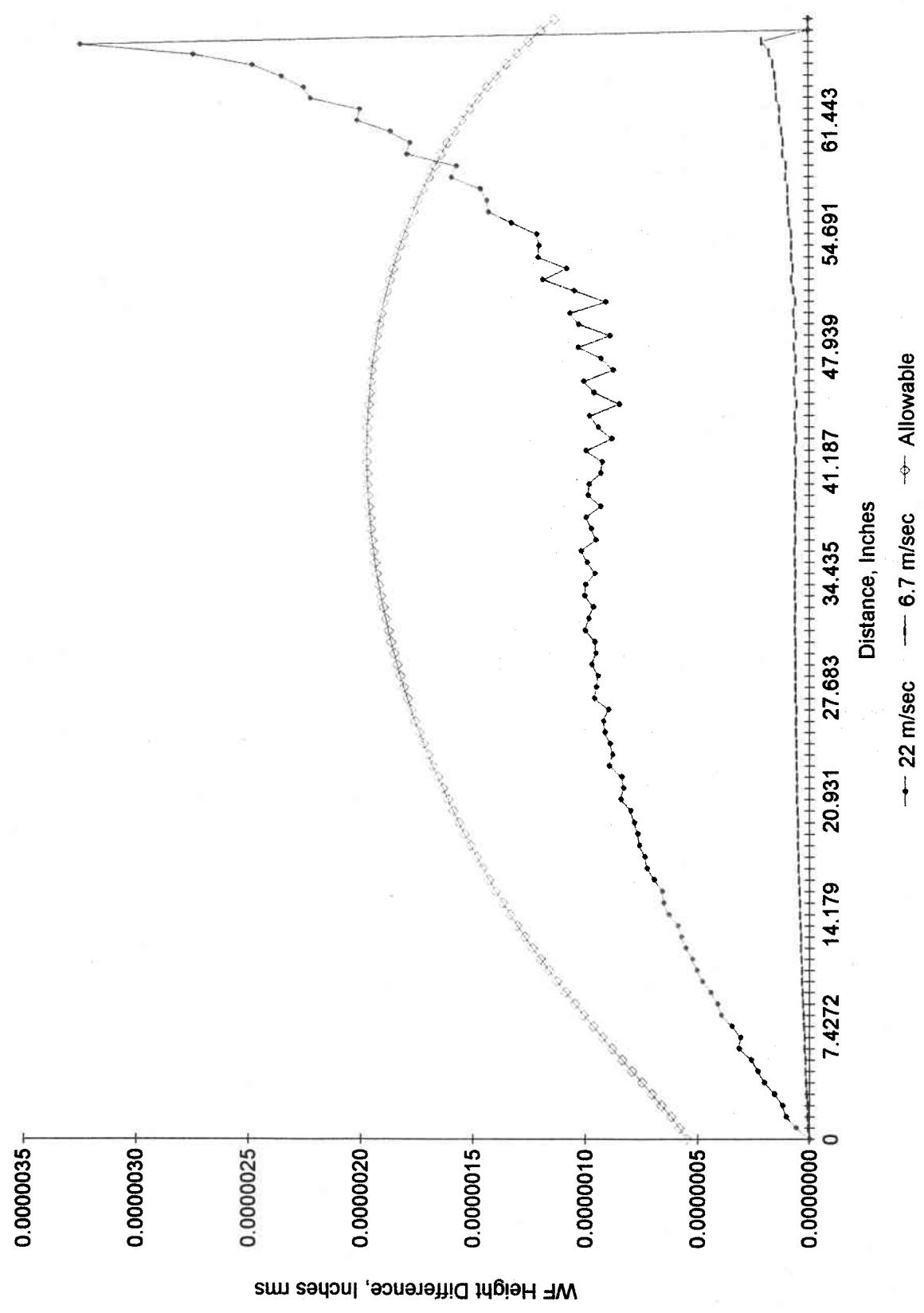


Figure G1 Structure Function, MMT f/5
 Wind Loading, Spts @30" Radius



APPENDIX H LOAD CASE LISTINGS

Secondary Characteristics Employed:

Best fit Radius (Rsph) = -206.57 inches
Clear Aperture = 0,33.5 inches

Available load cases are listed in this Appendix. Structure function files (.stf) have been copied into /home/bcuerden/mmt/f5sec/comb. The origination directory of these files is listed below.

chamfer/bcuerden/mmt/f5sec/f5sec

f5n36m xz symmetry, node file = f5sec.m15, Axials at 9.438, 19.594 and 30.8727

1. 1 g Z, 36 axials, uniform loads
2. 1 g Z, 36 axials, Fouter = 0.9*rest
3. 1 g Z, 36 axials, Fouter = 0.8*rest
4. 1 g Z, 36 axials, Fouter = 0.7*rest
5. 1 g Z, 36 axials, Fouter = 0.8*middle, Finner = 0.9* middle
6. 1 g Z, 36 axials, Fouter = 0.8*middle, Finner = 1.1* middle
7. 1 g Z, 36 axials, Fouter = 0.8*middle, Finner = 1.2* middle

dimension/d1/bcuerden/f5sec

f5sec full model, node file = f5sec.m15, Axials at 9.438, 19.594 and 30.11

- 1-6 1000 lb or in-lb Fr-Mz at 8322, Outer row of axials
- 7-12 1000 lb or in-lb Fr-Mz at 8551, Middle row of axials
- 13-18 1000 lb or in-lb Fr-Mz at 8778, Inner row of axials

f5secl full model, node file = f5sec.m15, Axials at 9.438, 19.594 and 30.11

- 1-6 1000 lb or in-lb Fx-Mz at 5134, Lateral Support
- 7-12 1000 lb or in-lb Fx-Mz at 5434, Lateral Support
- 13-18 1000 lb or in-lb Fr-Mz at 5363, Tangent Rods
- 19-24 1000 lb or in-lb Fx-Mz at 5126, Inner Row Lateral Support

dimension/d3/bcuerden/f5sec

f5latp yz symmetry, node file = f5sec.m15, Axials at 9.438,19.594,30.8727
Lateral supports displaced 0.050 toward face

1. 1 g Z on three fixed points at 30 R
2. Zenith to 30 degrees, 24 lateral supports
3. Zenith to 45 degrees, 24 lateral supports
4. Zenith to 60 degrees, 24 lateral supports
5. Zenith to 90 degrees, 24 lateral supports
6. Zenith pointing
7. Horizon pointing

f5latn Lateral supports at cg plane
y-z symmetry, node file = f5sec.m15, Axials at 9.438.,19.594,30.8727

1. 1 g Z on three fixed points at 30 R
2. Zenith to 30 degrees, 24 lateral supports
3. Zenith to 45 degrees, 24 lateral supports
4. Zenith to 60 degrees, 24 lateral supports
5. Zenith to 90 degrees, 24 lateral supports
6. Zenith pointing
7. Horizon pointing

f5latm yz symmetry, node file = f5sec.m15, Axials at 9.438,19.594,30.8727
Lateral supports displaced 0.050 toward back

1. 1 g Z on 3 fixed points at 30 R
2. Zenith to 30 degrees, 24 lateral supports
3. Zenith to 45 degrees, 24 lateral supports
4. Zenith to 60 degrees, 24 lateral supports
5. Zenith to 90 degrees, 24 lateral supports
6. Zenith pointing
7. Horizon pointing

f5astig Astigmatic load cases
x-z symmetry, node file = f5sec.m15, Axials at 9.438.,19.594,30.11

1. 1g Z on three fixed supports at 26 R
2. Unit astigmatic load on back supports
3. Unit astigmatic load on lateral supports

Table H.1 Detail List of Error Forces Verses Angle

Error Force Description	Error Force Magnitude for Indicated Orientation			
	Zenith	30 deg	45 deg	60 deg
Axial Support, Fr	0.1624	0.1406	0.1148	0.0812
Axial Support, Ft	0.1624	0.1406	0.1148	0.0812
Axial Support, Fz	0.1400	0.1400	0.1400	0.1400
Axial Support, Mr	0.3712	0.3215	0.2625	0.1856
Axial Support, Mt	0.3712	0.3215	0.2625	0.1856
Axial Support, Mz	0.4000	0.4000	0.4000	0.4000
Axial Locator, Fr	0.19	0.19	0.19	0.19
Axial Locator, Ft	0.19	0.19	0.19	0.19
Axial Locator, Fz	0.25	0.25	0.25	0.25
Axial Locator, Mr	0.90	0.90	0.90	0.90
Axial Locator, Mt	0.90	0.90	0.90	0.90
Axial Locator, Mzl	1.0	1.0	1.0	1.0
Lateral Support, Fx	0.0000	0.2795	0.3952	0.4841
Lateral Support, Fy	0.1268	0.1399	0.1453	0.1494
Lateral Support, Fz	0.0430	0.0954	0.1171	0.1337
Lateral Support, Mx	0.0570	0.0570	0.0570	0.0570
Lateral Support, My	0.0560	0.0560	0.0560	0.0560
Lateral Support, Mz	0.0000	0.2511	0.3549	0.4343
Lateral Locator, Fr	0.19	0.19	0.19	0.19
Lateral Locator, Ft	0.25	0.25	0.25	0.25
Lateral Locator, Fz	0.19	0.19	0.19	0.19

Lateral Locator, Mr	0.90	0.90	0.90	0.90
Lateral Locator, Mt	1.0	1.0	1.0	1.0
Lateral Locator, Mz	0.90	0.90	0.90	0.90
Orientation Angle, Deg.	0	30	45	60
Axial Loading (Axials)	23.2	20.0919	16.4051	11.6004
Lateral Loading	0	12.5563	17.7465	21.7154

APPENDIX I Lateral Support Interface to Mirror FEM

The stresses in the mirror and in the lateral support components were evaluated using the finite element model shown in Figures I.1 to I.4 . Stress results for the maximum 25 lb lateral force and for a 70 deg F temperature change are summarized in Table I.1 .

Table I.1 Summary of Stress Results, Lateral Support

Component	Stress Type	Loading	
		25 Lbs Fy	-70 deg F Change
Glass	σ_I or σ_{III} , psi	53.2	16.4
Silicone Adhesive	σ_{eqv} , psi	13.9	4.3
Bond Pad	σ_{eqv} , psi	266	51
Flexure Flanges	σ_{eqv} , psi	1095	115
Flexural Element	σ_{eqv} , psi	5895	2336
Beam	σ_{eqv} , psi	4001	283

Allowable Stresses:

Glass:	500 psi
Adhesive	90 psi
Metal Parts	8660 psi

Metal fatigue:

ASME BPVC for low strength carbon and low alloy steel = 13,000 psi
alternating stress for 10^6 cycles.

Allow a Kt of 3.0 and correct for non-reversing load:

$$\text{Metal stress allowable} = (2/3) * 13,000 = 8660 \text{ psi}$$

ANSYS 5.2
JUN 11 1997
13:41:15
PLOT NO. 2
ELEMENTS
TYPE NUM

XV =1
YV =1
ZV =1
DIST=7.622
VUP =Z
PRECISE HIDDEN

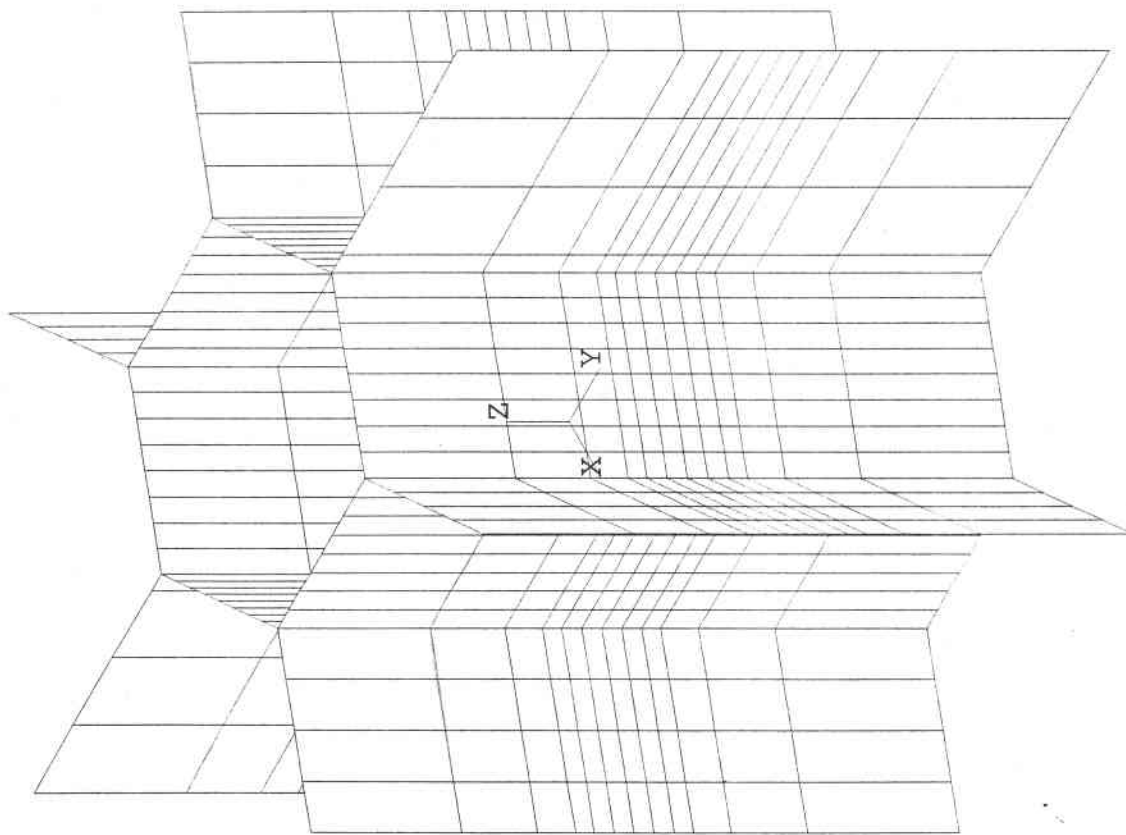


Figure I.1
MMT F5 Secondary Lateral Glass Interface Detail

ANSYS 5.2
JUN 11 1997
13:41:19
PLOT NO. 3
ELEMENTS
TYPE NUM

XV =1
YV =1
ZV =1
DIST=2.374
YF =-.6675
VUP =Z
PRECISE HIDDEN

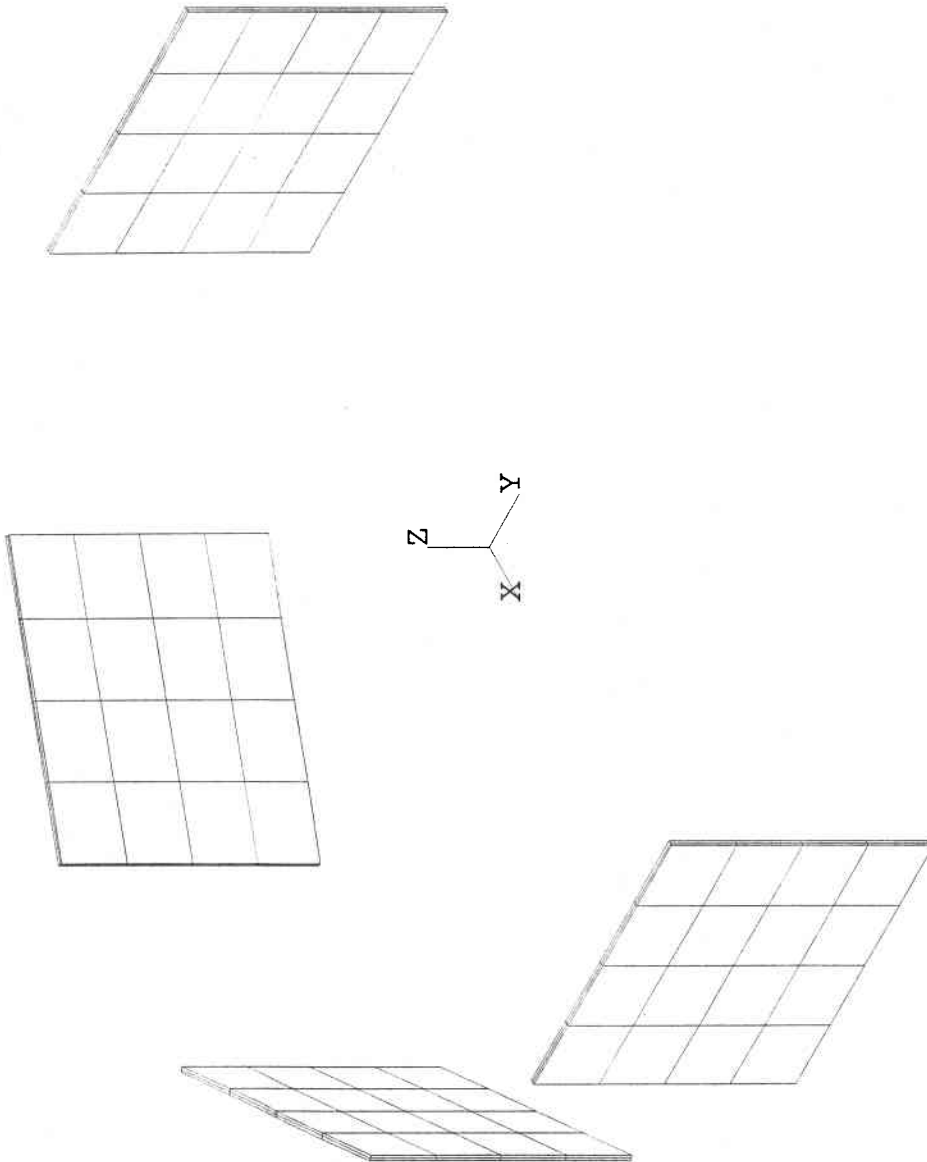


Figure I.2
MMT F5 Secondary Lateral Glass Interface Detail

ANSYS 5.2
JUN 11 1997
13:41:20
PLOT NO. 5
ELEMENTS
TYPE NUM

XV =1
YV =1
ZV =1
DIST=2.351
YF =-.658839
VUP =Z
PRECISE HIDDEN

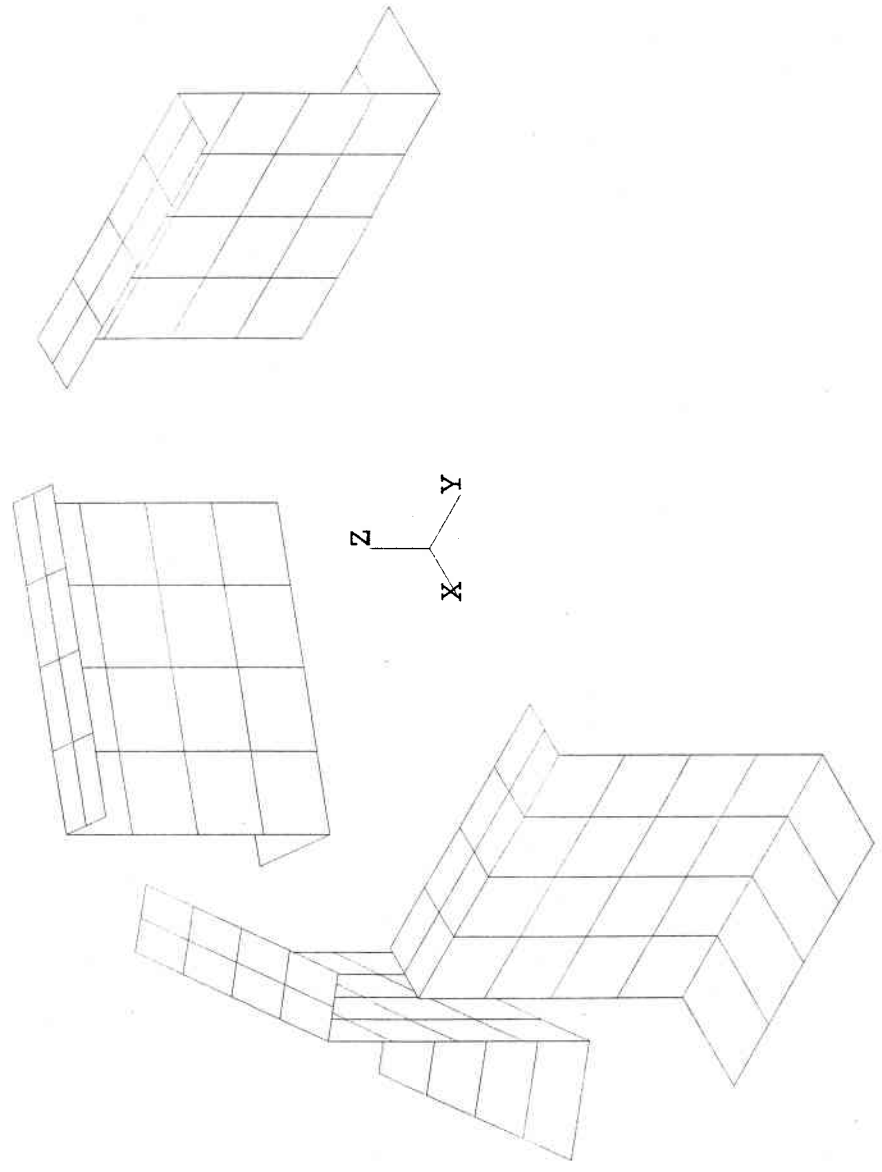


Figure I.3

ANSYS 5.2
JUN 11 1997
13:41:21
PLOT NO. 6
ELEMENTS
TYPE NUM

XV =1
YV =1
ZV =1
DIST=1.828
YF =-.2895
ZF =.25
VUP =Z
PRECISE HIDDEN

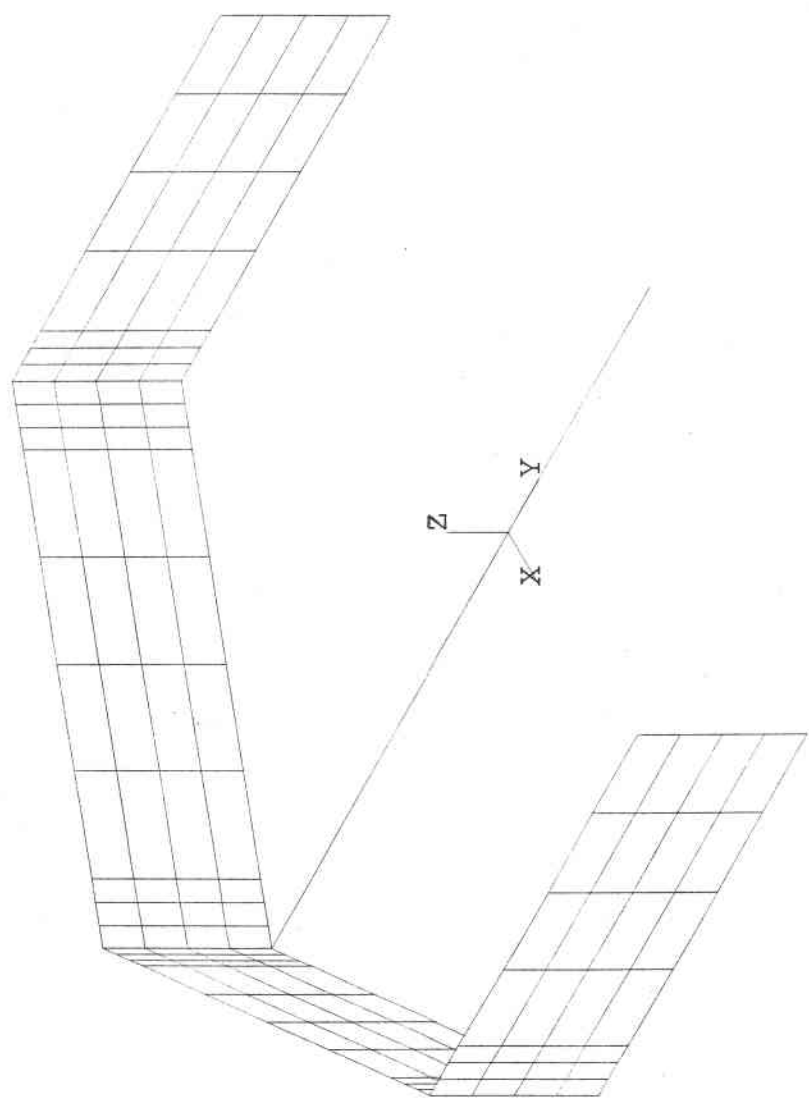


Figure I.4

MMT F5 Secondary Lateral Glass Interface Detail